Sperm derived H2AK119ub1 is required for embryonic development in *Xenopus laevis*

Valentin Francois--Campion[1,^], Florian Berger[1,^], Mami Oikawa[2], Maissa Goumeidane[1], Nolwenn Mouniée[1], Vanessa Chenouard[1], Kseniya Petrova[3], Jose G Abreu[3,4], Cynthia Fourgeux[1], Jeremie Poschmann[1], Leonid Peshkin[3], Romain Gibeaux[5], and Jérôme Jullien[1,*]

AFFILIATIONS

[1] Nantes Université, CHU Nantes, INSERM, Center for Research in Transplantation and Translational Immunology, UMR 1064, F-44000 Nantes, France

[2] Laboratory of Regenerative Medicine, Tokyo University of Pharmacy and Life Science, Hachioji, Tokyo, 192-0392, Japan

[3] Systems Biology, Harvard Medical School, Boston, MA, 02115, USA.

[4] Instituto de Ciências Biomédicas, Universidade Federal do Rio de Janeiro, Rio de Janeiro, RJ, 21941-590, Brazil

[5] Univ Rennes, CNRS, IGDR (Institut de Génétique et Développement de Rennes) - UMR 6290, F-35000 Rennes, France

^equal contribution

*Corresponding author email: jerome.jullien@inserm.fr

ABSTRACT [140words]

Deposition of H2AK119ub1 by the polycomb repressive complexe-1 plays a key role in the initiation of facultative heterochromatin formation in somatic cells. Here we evaluate the contribution of sperm derived H2AK119ub1 to embryo development. In *Xenopus laevis* we found that H2AK119ub1 is present during spermiogenesis and into early embryonic development, highlighting its credential for a role in the transmission of epigenetic information from the sperm to the embryo. *In vitro* treatment of sperm with USP21, a H2AK119ub1 deubiquitylase, just prior to injection to egg, results in developmental defects associated with gene upregulation. Sperm H2AK119ub1 editing disrupts egg factor mediated paternal chromatin remodelling processes. It leads to post-replication accumulation of H2AK119ub1 on repeat element of the genome instead of CpG islands. This shift in post-replication H2AK119ub1 distribution triggered by sperm epigenome editing entails a loss of H2AK119ub1 from genes misregulated in embryos derived from USP21 treated sperm. We conclude that sperm derived H2AK119ub1 instructs egg factor mediated epigenetic remodelling of paternal chromatin and is required for embryonic development.

INTRODUCTION

Several studies point towards an epigenetic contribution of sperm for embryonic development. First, in several species paternal exposure to various environmental insults results in changes to the offspring [1–5]. In addition to such environmentally induced epigenetic changes, sperm is also proposed to naturally harbour epigenetic cues that are required for development. Histones have been considered as possible vectors for such epigenetic information. Indeed, in several species including human, modified histones such as H3K4me3 and H3K27me3 are found in the sperm chromatin, in particular around developmental genes and in a pattern reminiscent of that found in embryonic stem cells[6–9]. In a previous work we provided evidence that in the frog, *Xenopus laevis,* some of these modified histones are homogenously distributed in a population of sperm cells, hence indicating that they have the required attributes for a role in the regulation of embryonic development[10]. Lastly, interference with histone variant or post-translational modifications during the formation of the gametes, or after fertilisation, lead to embryonic gene misregulation[9,11,12]. Although these later experiments support a functional role for sperm-derived modified histone in embryonic development, indirect effect of the interference on the process of spermiogenesis or early embryos development cannot be ruled out. A direct assay to test for the requirement of sperm modified histones in embryo development is still lacking. This is due in part to the difficulty to access the chromatin in the highly compacted sperm nucleus. In this work, we aim to fill this gap and devised a strategy to alter the sperm epigenome just prior to its introduction to the egg. We specifically considered H2AK119ub1 as a possible carrier of necessary epigenetic information from the sperm to the embryos. Indeed, recent works points towards a key role of polycomb repressive complexe-1 (PRC1), upstream of PRC2, in the establishment of facultative heterochromatin, both in cultured cells and in embryos[13]. The H2AK119 ubiquitylation activity of the PRC1 complex appears to be integral part of this mechanism[13,14]. In *Xenopus laevis* we found that H2AK119ub1 dynamic during spermiogenesis and early embryonic development is compatible with a role in the epigenetic programming of sperm for embryonic development. We applied an *in vitro* epigenetic editing assay that uses USP21 deubiquitylase activity [15–18] to erase H2AK119ub1 from sperm chromatin. Embryos derived from such epigenetically edited sperm are developmentally impaired. Transcriptome and epigenome analysis indicates that H2AK119ub1, in combination with H3K4me3, is enriched on a set of embryonic genes misregulated in embryos derived from USP21 treated sperm. Such USP21 sensitive genes preferentially retain H2AK119ub1 upon sperm chromatin exposure to maternal factors. Lastly, we provide evidence that egg factor mediated deposition of H2AK119ub1 on paternal chromatin is influenced by pre-existing sperm H2AK119ub1.We conclude that sperm derived H2AK119ub1 instructs egg factor mediated epigenetic remodelling of paternal chromatin and is required for embryonic development.

RESULTS

We first evaluated the overall levels of H2AK119ub1 in chromatin during spermiogenesis and early embryonic development. Indeed, the presence of such modified histone in sperm seems to differ between species, its presence documented in that of mouse[19] while it appears absent in that of zebrafish[20]. In frogs the last stage of spermatogenesis is associated with a remodelling of nucleosomes resulting in a partial loss of H2A/H2B while a full complement of H3/H4 is retained on sperm chromatin

(**Fig. 1A**)[10]. Western Blot (WB) analysis captures this loss of H2A and reveal an overall decrease in H2AK119ub1 in sperm compared to spermatid (**Fig. 1B and Suppl Fig.S1-A**, see H2A/H4 and H2AK119ub1/H4 ratio, respectively). Importantly however, the H2AK119ub1 to H2A ratio is similar in sperm compared to spermatid, indicating that in this context of spermiogenesis-associated H2A loss, a significant level of H2AK119ub1 is maintained in sperm (H2AK119ub1/H2A, **Fig. 1B**). We next assessed H2AK119ub1 occurrence after fertilisation: in early frog embryos around ZGA (blastulae stage) and later during gastrulation and neurulation. Interestingly, contrary to what is seen with H3K27me3, a PRC2 associated modification, H2AK119ub1 is detected throughout early embryogenesis (**Fig. 1C**). Altogether, these observations highlight H2AK119ub1 credentials for a potential role in the transmission of epigenetic information from sperm to the embryos.

We then carried out H2AK119ub1 ChIP to map the distribution of this histone post-translational modification (PTM) on the sperm genome. Biological triplicates were well correlated and subsequently pooled for downstream analysis (**Suppl Fig. 2A-D**). We first assessed the distribution of H2AK119ub1 around the transcription start of all sperm genes. H2AK119ub1 accumulates around the TSS of a fraction of sperm genes (**Fig. 2A**), similar to what is observed in somatic cells[21] and embryos[14,20]. Noticeably, we observed in the top 10% TSS harbouring H2AK119ub1 an enrichment for genes associated with developmental function (**Fig. 2A, Suppl Table 1**), and reminiscent of the association reported with H3K27me3 in many species[6–9]. We next sought to more generally identify regions associated with H2AK119ub1 genome wide. H2AK119ub1 is a pervasive histone modification typically present on ~10% of nuclear H2A in somatic cell[22,23] and up to ~40% in germ cells[19]. In *Xenopus laevis* sperm, it accumulates over region covering larger part of the genome than other modified histones with broad distribution such as H3K27me3 (**Suppl Fig. 2E**). To identify region of H2AK119ub1 genomic enrichment we therefore used RECOGNICER, a coarse-graining approach designed to capture enrichment over broad scale[24] (**Suppl Fig. 3, Table S1**). Although we observed peaks of accumulation around genes, such as illustrated for *wnt1.L*, *pax6.L* or the *hoxa.S* cluster (**Fig. 2B)**, a large proportion of H2AK119ub1 also accumulates on the sperm genome in distal region away from genes (**Fig. 2C**). Noticeably we observed that H2AK119ub1 is significantly associated with sperm gene regulatory elements (promoters and enhancers, **Fig. 2D**). Epigenetic control of gene expression often entails a combination of epigenetic cues such as those observed in X inactivation[25] or in transcriptional reprogramming[26]. We therefore investigated the relationship between genomic regions enriched in sperm for H2AK119ub1 and for other histone post-translational modifications. We focused on H3K27me3[10], associated with the activity of Polycomb Repressive Complex 2, and H3K4me3[10], a histone modification associated with transcription (Peaks, *e.g.* around *pax6.L* and *hoxa.S* loci, **Fig. 2B**). We then determined the genome-wide association of H2AK119ub1 with methylated K4 and/or K27 on histone H3. While most H2AK119ub1 peaks exist independently of these methylated histones, ~24% of H2AK119ub1 peaks overlap with either H3K4me3 and/or H3K27me3 peaks (**Fig. 2E**). We observed a very strong promoter bias for peaks of H2AK119ub1 co-occurring with H3K4me3, an expected trend given that H3K4me3 is known to strongly associate with gene promoter (**Fig. 2F**). By contrast, when occurring in the absence of H3K4me3, H2AK119ub1 is located away from promoter and in intergenic regions. Analysis of fragment length obtained following sequencing of ChIP and Input fractions allow the discrimination of DNA fragment associated with nucleosomes (full complement of

138 histones protecting 150bp of DNA) from those associated with subnucleosomes
139 (nucleosomes lacking one or two H2A-H2B dimer and protecting 110 or 70bp of
140 DNA) in sperm chromatin (**Suppl Fig. 4**). Noticeably, in sperm chromatin on the whole,
141 H2AK119ub1 is mostly associated to nucleosomes while H3K27me3 and H3K4me3
142 tend to be associated with subnucleosomes. So, while we observe co-enrichment of
143 H2AK119ub1 with methylated histone H3 at a subset of genomic loci, those histone
144 modifications are possibly present at those sites on adjacent
145 nucleosomal/subnucleosomal nucleoprotein complexes rather than on the same particle.
146 Altogether, this survey of H2AK119ub1 distribution in sperm reveals its enrichment on
147 gene regulatory region further strengthening its potential for gene regulation across
148 generation.

149 To further evaluate how sperm H2AK119ub1 could have an impact on
150 embryonic development, we next sought to follow its fate after fertilisation. Following
151 delivery to the egg, protamines are removed from sperm chromatin and a canonical
152 nucleosomal structure is re-instated. In conjunction with these events the sperm
153 chromatin is replicated. Therefore, the extensive changes to sperm chromatin that
154 follow fertilization have the potential to profoundly alter the sperm derived modified
155 histone landscape. To determine the fate of sperm modified histones we turned to
156 interphase egg extracts that can mimic the sperm chromatin remodelling events that
157 follow fertilization, including protamine to histone transition and DNA replication[10].
158 We carried out H2AK119ub1 and H3K4me3 ChIP-seq on untreated sperm, or sperm
159 having gone through egg extract mediated replication (**Fig. 3A**). Combining this dataset
160 with existing spermatid and gastrulae ChIP-seq[9,10,27] we obtain a global view of
161 H2AK119ub1, H3K4me3, and H3K27me3 dynamic during spermiogenesis and early
162 embryogenesis (**Fig. 3B**). Remarkably, while H3K4me3 and H3K27me3 are mostly
163 stable, H2AK119ub1 exhibits drastic redistribution throughout this developmental
164 period. Indeed, a large set of genomic location acquires H2AK119ub1 following sperm
165 chromatin replication (cluster 4, **Fig. 3B, Suppl Table 2**), and includes a large
166 proportion of gene TSSs (**Suppl Fig. 5A**). To better delineate the principle of this
167 developmental dynamic, we then compared H2AK119ub1 and H3K4me3 peaks in
168 untreated (sperm) *versus* egg extract treated sperm (replicated sperm). We confirm a
169 marked disparity in replication dynamics between sperm H3K4me3, mostly stable
170 (77% of sperm peaks conserved after replication (19345/24982) and 52% stable peaks
171 overall (19345/36770)), and sperm H2AK119ub1, mostly changing (23.5% of sperm
172 peaks maintained after replication (15796/67233) and 15% stable peaks overall
173 (15796/108740)) (**Fig. 3C, Suppl Fig. 5B)**. Most of the replication redistribution of
174 H2AK119ub1 happens in intergenic region, while H2AK119ub1 peaks stable through
175 this process are mostly located on promoter (**Suppl Fig. 5D**). In this dynamic landscape,
176 the subset of H2AK119ub1 genomic location associated with H3K4me3 in sperm
177 appears selectively conserved (93% of sperm bivalent peaks are maintained after
178 replication (5222/5597) (**Fig. 3C**). Broader H2AK119ub1 peaks with higher level of
179 H2A retention discriminate location where H2AK119ub1/ H3K4me3 is maintained
180 following exposure to egg factors from those where it is lost (**Suppl Fig. 5C**). Lastly,
181 we confirmed that the H2AK119ub1 configuration observed following *in vitro*
182 treatment of sperm with egg extract is also detected in blastulae stage embryo at the
183 time of ZGA (**Suppl Fig. 6A-C**). We conclude that sperm exposure to egg factors
184 profoundly remodels paternal H2AK119ub1 genomic distribution.

185 We next evaluated to which extent such egg factor-mediated H2AK119ub1
186 remodelling is dependent on incoming sperm chromatin component. To directly

evaluate sperm H2AK119ub1 functional relevance to this process, we set out to erase this histone modification, after completion of spermatogenesis, and prior to exposure to egg factors. To that end, we incubated mature sperm in an oocyte extract containing USP21, a H2A deubiquitylase[15,28] (**Fig. 4A**). In such extract, the sperm nucleus is partially decondensed, allowing efficient deubiquitylation of H2AK119ub1 while the levels of trimethylated H3K4, H3K9 and H3K27 remain unchanged (**Fig. 4B, Suppl Fig. 7A, Suppl Fig. 1B**). Importantly, MNAse digestion of oocyte extract USP21-treated sperm yields nucleosomal and subnucleosomal size DNA fragments typical to that of naïve *Xenopus* sperm[9] (**Fig. 4C**, **Suppl Fig. 7B, and 7C left**). This indicates that the overall sperm chromatin structure is maintained after oocyte extract treatment and does not convert to a somatic type of chromatin organisation as triggered by egg extract treatment[29] (**Fig. 4C, Suppl Fig. 7**). We next asked to what extend USP21 mediated erasure of H2AK119ub1 from sperm chromatin influences its egg factor mediated redistribution. To that end, we carried out modified histone analysis in sperm treated with control or USP21 extract oocyte with or without a subsequent incubation in egg extract (**Suppl Fig. 8A**). Interestingly, WB analysis indicates that H2AK119ub1, erased from sperm chromatin by USP21 treatment, is at least partially reinstated by subsequent exposure to egg extract (**Fig. 4D**), indicating the existence of a maternal H2AK119 ubiquitylation activity independent of pre-existing sperm H2AK119ub1. Using ChIP-seq, we next ask if sperm H2AK119ub1 erasure prior to exposure to egg components affects the maternal factor mediated remodelling of H2AK119ub1 on paternal chromatin. We first focused on sperm genomic sites where we previously detected accumulation of H3K4me3, H3K27me3, or H2AK119ub1 (as in **Fig. 3B)**. This analysis confirmed that USP21 efficiently erases H2AK119ub1 from its genomic site in sperm (**Suppl Fig. 8B, Suppl Table 3**). We observed an overall reduction in egg factor mediated H2AK119ub1 deposition on chromatin derived from USP21+ sperm compared to that from USP21-sperm (**Suppl Fig. 8B**). We then compared H2AK119ub1 peaks in samples originating from replicated USP21-treated sperm to that from replicated control-treated sperm (**Fig. 4E**). Surprisingly, we observed that sperm USP21 treatment leads not only to loss of H2AK119ub1 peaks post-replication (lost peaks) but also triggers the appearance of a large set of peaks that is not deposited by maternal factors in control sperm samples (gained peaks) (**Fig. 4E**). Comparatively, USP21 treatment impact on post-replication H3K4me3 is much milder (**Suppl Fig. 8C**). To better characterize this shift, we first evaluated if H2AK119 ubiquitylation sites detected following egg extract exposure of sperm harbour genomic features associated with variant PRC1 (vPRC1) targeting in somatic cell (reviewed in[30]). Those H2AK119ub1 sites that are specific to egg extract treated control sperm (lost peaks, **Fig. 4E**) are associated with cluster 4 in Fig.3B and are indeed enriched for TF motifs associated with vPRC1 targeting (*i.e.* USF1/2 E2F, E-box, **Suppl Fig. 8D, Suppl Table 2**). We also detected a strong association of these sites with unmethylated CpG island (**Fig. 4F-G**), a genomic feature also shown to attract vPRC1 activity. By contrast, sperm treatment with USP21 prior to egg factor exposure redirects H2AK119ub1 accumulation towards repeat elements and away from such targets (**Fig. 4H-I, Suppl Fig. 9, Suppl Table 5**). We conclude that maternal factors mediated redistribution of sperm H2AK119ub1 is instructed by pre-existing H2AK119ub1 derived from paternal chromatin. In the absence of sperm H2AK119ub1, maternal factor mediated H2A ubiquitylation activity is shifted from CpG islands to repeat elements.

To then determine the functional relevance of sperm derived H2AK119ub1 to embryo development, we took advantage of the availability of paternally derived

236 embryos in frog. As described previously, such embryos develop solely on chromatin
237 derived from sperm and provide a direct measure of the paternal contribution to early
238 development[9]. We generated paternally derived embryos from sperm pre-incubated in
239 control or USP21 containing oocyte extracts and monitored their development (**Fig.**
240 **5A**)[31]. From gastrulation onwards, we observed a decrease in the developmental
241 potential of USP21 treated- compared to control treated- sperm derived embryos (**Fig.**
242 **5B**). We conclude that besides its DNA content, sperm also contributes to the embryo
243 an USP21 sensitive signal that is necessary for development. The observed defects
244 occur around the time of zygotic gene activation suggesting that USP21 treatment
245 associated developmental failure might relate to defective regulation of embryonic gene
246 expression. To evaluate this possibility, we carried out transcriptome analysis of early
247 gastrulae generated from pool of untreated, control extract-treated or USP21 extract-
248 treated haploid embryos. We performed RNA-seq analysis using sperm, oocyte extract,
249 and egg originating from different preparations for each of the biological replicates.
250 Differential gene expression analysis indicates that the treatment of sperm with a
251 control oocyte extract has minor effect on the resulting embryo transcriptome when
252 compared to embryos generated from untreated sperm (**Fig. 5C**, left; **Suppl Fig. 10A-**
253 **B**). By contrast, USP21 extract treatment leads to embryonic misregulation of 269
254 genes (**Fig. 5C**, right), the majority of which are upregulated in embryos derived from
255 USP21 extract treated sperm compared to embryos derived from control extract treated
256 sperm (74%, 200/269, **Fig. 5D, Suppl Fig. 10C, Suppl Table 4**). Thereafter, this set of
257 genes found differentially expressed in embryos derived from sperm treated with
258 USP21 oocyte will be referred to as USP21 sensitive genes. GO enrichment analysis
259 highlight genes related to cell cycle processes in this gene set (**Suppl Table 4**). We next
260 asked to which extend the expression pattern of USP21 sensitive genes identified on
261 pooled embryos reflect the behaviour in single embryos. To that end, we carried out
262 transcriptome analysis in single paternally derived gastrulae. We find that the
263 expression pattern of USP21 sensitive gene observed in pooled embryos is replicated
264 in half of the single embryos derived from USP21-treated sperm (4/8 USP21 treated
265 sperm derived embryos, **Suppl Fig. 10D**). This heterogeneous transcriptome pattern
266 matches the observed developmental outcome, with a fraction of gastrulae derived from
267 USP21-treated sperm developing to the tadpole stage (**Fig. 5B)** and is reminiscent of
268 the transcriptome heterogeneity detected in cloned embryos[32]. We then interrogated the
269 developmental dynamic of USP21 sensitive genes. We observed a clear distinction
270 between up- and down regulated USP21 sensitive genes (**Suppl Fig. 10E**). During
271 development of embryos generated by *in vitro* fertilisation[33], upregulated genes exhibit
272 a strong maternal contribution followed by clearing prior to gastrulation (stage 10-12)
273 and re-expression at tadpole stage (stage 25-40) while downregulated genes show
274 increased expression around gastrulation. A recent study indicates that at ZGA,
275 transcription occurs on genes with (maternal-zygotic, "MZ genes") or without (zygotic,
276 "Z genes") a maternal contribution of transcripts[34,35]. Interestingly, we observed that
277 USP21 sensitive genes are enriched for MZ genes, indicating that these genes exhibit
278 zygotic transcription in the context of a maternally derived transcripts (**Suppl Fig. 10E-**
279 **F)**. Taken together, these analyses support the hypothesis whereby USP21 mediated
280 erasure of the repressive histone modifications H2AK119ub1 from sperm leads to
281 precocious embryonic expression of a subset of genes that could in turn impact critical
282 embryonic process such as cell division.

283 To evaluate this possibility further, we investigated to which extent
284 H2AK119ub1 genomic distribution associate with embryonic gene sensitivity to sperm

285 USP21 treatment. We observed an enrichment of sperm H2AK119ub1 peaks on USP21
286 sensitive gene body (**Suppl Fig. 10G**). Additionally, using a genome partitioning
287 approach (hidden Markov model) we also observe that USP21 sensitive genes are
288 associated with genomic regions exhibiting H2AK119ub1 either in sperm or in sperm
289 following exposure to egg extract (**Suppl Fig. 10H).** However, many more genes
290 harbour this modification in sperm, without being affected by USP21 treatment. We
291 therefore next interrogated the association of USP21 sensitive genes with different
292 types of H2AK119ub1 peaks stratified according to association with other histone
293 PTMs, namely H3K4me3 and H3K27me3 (as in **Fig. 2E-F**). We detect an association
294 of USP21 sensitive gene features with either H2AK119ub1 only peaks
295 (H2AK119ub1+; H3K4me3-; H3K27me3-) or trivalent H2AK119ub1 peaks
296 (H2AK119ub1+; H3K4me3+; H3K27me3+) (**Fig. 6A**). Strikingly however, USP21
297 sensitive genes show a strong enrichment for bivalent H2AK119ub1/H3K4me3 and
298 depletion for bivalent H2AK119ub1/H3K27me3 chromatin configuration. This
299 analysis suggests that the effect on embryonic gene expression of sperm USP21
300 treatment arise from erasure of H2AK119ub1 in the context of a bivalent
301 H2AK119ub1/H3K4me3 chromatin status. We also observed that, post-replication,
302 H2AK119ub1 and H3K4me3 signals around USP21 sensitive gene TSSs are higher
303 than around the bulk of *X. laevis* genes TSSs (**Fig. 6B**). Importantly, the significant
304 enrichment of USP21 sensitive genes promoter and gene body for a bivalent
305 H2AK119ub1/H3K4me3 chromatin configuration reported in sperm holds true after
306 sperm replication (**Suppl Fig. 10I**). This association of USP21 sensitive genes with
307 H2AK119ub1 is also observed in embryos at ZGA, with such trend still present but less
308 pronounced later during embryogenesis (**Suppl Fig. 6D**). We then took advantage of a
309 published dataset describing the consequences of expressing the H2A deubiquitylase
310 BAP1 in early mouse embryos to investigate if such a relationship is conserved across
311 specie[19]. Using a hidden Markov model, we indeed found that gene identified as
312 BAP1 sensitive in mouse two cell embryos are enriched in genome domains
313 exhibiting H2AK119ub1 marking in sperm (**Suppl Fig. 10J-K**). Altogether these
314 observations support a role for sperm derived H2AK119ub1 in the regulation of the
315 expression of a subset of embryonic genes.

316 We next considered the possibility that while a local accumulation of
317 H2AK119ub1 could be maintained post-replication, sperm modified histones could
318 have undergone replicative dilution. In other word, during replication the local
319 accumulation of histone along the genome could be maintained albeit at a reduced level,
320 for example through redistribution of sperm derived modified histones between the
321 replicated strands of DNA. Mechanistically, this is important as in frog ~8 rounds of
322 replication separate fertilisation form the main wave of ZGA and could therefore leads
323 to complete loss of sperm derived modified histones. Therefore, to compare
324 H2AK119ub1 level pre- and post- replication we calibrated the signal *via* semi-
325 synthetic H2AK119ub1 nucleosome spiked-in used in the ChIP-seq (see M&M)
326 (**Fig.6C**). We observed a global decrease of H2AK119ub1 signal on TSSs upon egg
327 extract treatment, suggesting that sperm chromatin replication induces redistribution of
328 this modified histones at these locations (black line, **Fig. 6C**). When considering USP21
329 sensitive gene however, we observed a different trend. While an overall decrease of
330 H2AK119ub1 signal is also detected upon replication, H2AK119ub1 loss is clearly less
331 pronounced on the TSSs of this subset of gene than seen genome wide (red line, **Fig.**
332 **6C),** a feature shared with the broader set of gene that have maternal-zygotic
333 contribution (green line, **Suppl Fig. 10L**). These analyses indicate that USP21 sensitive

genes are indeed associated with a sperm H2AK119ub1 configuration that persists through egg factor mediated remodelling of the paternal epigenome. Lastly, we asked how sperm USP21 treatment induced disruption of paternal epigenome remodelling by egg factors affects USP21 sensitive genes. We found that the shift of H2AK119ub1 away from CpG towards repeat elements induced by USP21 treatment (as in **Fig. 4E**) significantly deplete post replication association of USP21 sensitive genes from this histone modification (**Fig. 6D**). Analysis of gene TSSs also showed that the preferential post replication retention of H2AK119ub1 on USP21 sensitive genes is lost in response to H2AK119ub1 sperm editing (**Fig. 6E**).

Taken together our results reveal that the setup of paternally derived zygotic chromatin is dictated by component of the sperm epigenome and that this process is required for proper expression of a subset of embryonic genes.

DISCUSSION

In this work, we found that in *Xenopus laevis*, paternal H2AK119ub1 genomic distribution is extensively remodelled upon exposure to egg factors, reminiscent of the situation found in the mouse[19]. In this dynamic epigenetic landscape, a subset of genomic location is nevertheless found to maintain H2AK119ub1 following sperm replication in extract as well as following early embryonic division. This suggests that the mechanism recently described in cultured cells and demonstrating recycling of H2AK119ub1 between daughter cells[67] could apply to the transmission of H2A associated epigenetic cue from the gametes to the dividing cell of the frog embryos. Besides those stable sites of H2AK119ub1 accumulation, sperm incubation in egg extract also triggers H2AK119ub1 deposition on new genomic sites. Whether this remodelling requires replication is not known since sperm treatment with egg extract triggers many processes besides replication. Once established those new sites appear stable through replication as they could be detected in late cleavage stage embryos. However, our study is limited by the lack of knowledge about H2AK119ub1 genomic distribution during xenopus laevis pre-ZGA developmental period. Particularly, we are lacking in vivo data describing the H2AK119ub1 landscape immediately after fertilisation and during the first round of embryonic divisions. Therefore, mechanistically we don't know if the remodelled H2AK119ub1 distribution found after in vitro sperm replication, and in vivo after 8 round of cell division, is faithfully transmitted throughout cleavage stage or transiently adopt a different configuration during that period.

Egg factor dependent accumulation of H2AK119ub1 occurs around unmethylated CpG island and/or TF binding sites (*i.e.* USF1/2), genomic features that are known target of PRC1 activity in other systems[30]. Besides transcription factors, Kdm2b a component of vPRC1 is involved in more broadly targeting the H2AK119 ubiquitylation activity of this complex to unmethylated CpG island in ESC[30]. Kdm2b is a likely candidate for a role in the observed H2AK119ub1 remodelling following exposure to egg components as it is maternally provided as protein in frog (https://www.xenbase.org/xenbase/gene/geneExpressionChart.do?method=drawProtein). In mouse embryonic stem cell, the establishment of polycomb repressive domain occurs in a stepwise manner with a variant PRC1 complex initiating their

380 formation through ubiquitylation of H2AK119, followed by recruitment of the PRC2
381 complex and subsequent methylation of H3K27me3. Such sequential events have also
382 been described during Neural Progenitor Cell differentiation[36] and X chromosome
383 inactivation[37]. Recently, this sequence of events have been investigated in the mouse
384 and zebrafish embryos[19,20,38]. In these embryos H2AK119ub1 is also required for the
385 deposition of H3K27me3 and transcriptional repression around the time of zygotic gene
386 activation. Our observation that H2AK119ub1 is present in pre-ZGA embryo in the
387 absence of H3K27me3 argues for the existence of a similar mechanism in frog[39,40].

388 Interference with H2AK119ub1 in the mouse, either by knocking down PRC1
389 component[38] in oocyte, or erasing H2AK119ub1 from embryos[19,20] leads to mis-
390 regulation of genes at ZGA and is associated with embryonic lethality. While clearly
391 demonstrating a role for H2AK119ub1 in regulation of transcription around ZGA, these
392 approaches entail prolonged epigenetic interference during either gametogenesis or
393 early embryogenesis and, as a consequence, do not enable to determine the extent to
394 which embryonic H2AK119ub1 is instructed/inherited from sperm and/or oocyte
395 H2AK119ub1[9,11,12,19,20,38]. Here, by editing the sperm epigenome, after completion of
396 spermiogenesis and prior to exposure to egg factors, we circumvent these limitations.
397 We demonstrate that sperm contribute to the embryo a USP21 sensitive cue required
398 for paternal H2AK119ub1 remodelling by egg factor, embryonic gene expression, and
399 developmental competence (**Fig. 7**). We find that egg factor mediated accumulation on
400 paternal CpG island depends on H2AK119ub1 delivered by the sperm. Strikingly, we
401 observe that erasure of H2AK119ub1 from sperm leads to a global shift in genomic
402 accumulation from CpG islands to repeat elements. Given the propensity of vPRC1 to
403 be targeted to and to spread from existing H2AK119ub1 location[41] it raises the
404 possibility that pre-existing sperm derived "docking sites" could limit chromatin
405 sampling by the polycomb complex and prevent H2AK119ub1 deposition at genomic
406 location where targeting is usually limited such as the repeat elements. Embryos
407 derived from H2AK119ub1 edited sperm exhibit transcriptional misregulation, mostly
408 upregulation, compatible with the repressive function of this histone PTM on
409 transcription. A similar observation is observed in mouse when H2AK119ub1
410 deubiquitylase is expressed at fertilization[19], or in zebrafish when Rnf2 is chemically
411 inhibited[20]. Given the extent of egg factor mediated H2AK119ub1 accumulation on
412 gene promoters observed in frog, mouse or zebrafish, it is somewhat surprising that
413 only a limited number of genes are mis-regulated when its distribution is massively
414 altered. We identify an association of misregulated genes with H2AK119ub1 in frog
415 sperm and find that this association is preferentially maintained on these genes upon
416 sperm chromatin replication, further supporting a direct role for this histone post-
417 translational modification in the epigenetic programming of sperm for regulation of
418 embryonic transcription. We cannot rule out that a part of the genes is indirectly
419 affected, for example as downstream target of a "primary" H2AK119ub1 target.
420 Alternatively, we provide evidence that gene sensitivity to H2AK119ub1 erasure from
421 sperm occurs when genes are associated with H3K4me3, a histone PTM known to act
422 as a vector of intergenerational information[9–11,42,43]. It is likely that additional epigenetic
423 features besides H3K4me3 contribute to gene sensitivity to H2AK119ub1 erasure from
424 sperm. Additionally, we observe that most affected genes are normally expressed late
425 in embryogenesis (tadpole stage) a feature also seen in mouse with a large proportion
426 of gene sensitive to H2AK119ub1 depletion expressed post-implantation[8]. It is
427 therefore possible that the effect of H2AK119ub1 expression is only partially revealed

428 at early embryonic stage since transcription factors targeting these genes might not be
429 present.

430 Our work advance knowledge form previous studies by showing that part of
431 H2AK119ub1 found in embryos is paternally instructed. This necessary function of
432 sperm derived modified histones has important bearing on our understanding of
433 inter/trans generational transmission of epigenetic information. One could
434 indeedenvisage that such a naturally occurring mechanism of epigenetic information
435 transmission to the embryos could be hijacked to transmit environmentally induced
436 sperm epigenetic cues. Based on the very dynamic nature of histone PTMs around
437 fertilisation, it is likely that transmission to the embryos will be context- (combination
438 of marks) and location- dependent. Future studies will aim at evaluating to which extent
439 sperm histones PTMs differ between individuals and to which extent they are
440 maintained in embryos.

441

442

443 **FIGURE LEGENDS**

444 **Figure 1**: ***H2AK119ub1 dynamics during spermiogenesis and early embryonic***
445 ***development***

446 (**A**) Schematic representation of *Xenopus laevis* nucleosome remodelling during
447 spermiogenesis (**B**) Left, Western blot analysis of H2AK119ub1, H2A and H4 histones.
448 Right quantitation of signal ratio of H2A to H4, H2AK119ub1 to H4, and H2AK119ub1
449 to H2A, in spermatid and sperm. * $p<0.05$, ratio paired t test (n=4). Median is shown.
450 (**C**) Western blot analysis of H2AK119ub1, H3K27me3, H3K9me3, H3K4me3, H3 and
451 H4 in *Xenopus laevis* embryo pre- (blastulae) and post- (gastrulae, and neurula) ZGA.

452

453 **Figure 2**: ***H2AK119ub1 associates with gene regulatory regions in sperm chromatin***

454 **(A)** Heatmap of H2AK119ub1 signal (log(ChIP/Input)) on all *Xenopus laevis* genes
455 TSS +/-5kB. GO enrichment is shown for the top 10% genes. **(B)** Genome browser
456 view of log(ChIP/Input) of sperm H2AK119ub1, H3K4me3, and H3K27me3 around
457 *wt1.L, pax6.L*, *snx10.s* and *hoxa.S* loci. Boxed area underneath the gene track indicates
458 regions of enrichment (peaks). **(C)** Distribution of sperm H2AK119ub1 peaks on
459 genomic features. **(D)** Fold enrichment of H2AK119Ub1 peaks on different genomic
460 features, *** $p<0.001$, permutation test. **(E)** Pie chart indicating the proportion of
461 H2AK119ub1 peaks either alone, or overlapping H3K4me3 and/or H3K27me3 peaks
462 in sperm. **(F)** Genomic distribution of sperm H2AK119ub1 peaks according to overlap
463 with H3K4me3 and/or H3K27me3 peaks.

464

465 **Figure 3:** ***Sperm H2AK119ub1 is remodelled following exposure to egg factors***

466 **(A)** Experimental design for monitoring modified histones fate following sperm
467 exposure to egg factors. (**B**) Heatmap of H2AK119ub1, H3K4me3, or H3K27me3
468 signal (log(ChIP/Input)) in spermatid, sperm, replicated sperm, and gastrula. All

genomic locations enriched for one of these histone modifications (peaks) in at least one of these developmental stages are represented. **(C)** Venn diagram indicating the changes to H2AK119ub1 (left), H3K4me3 (middle) or overlapping H3K4me3/H2AK119ub1(right) peaks during sperm chromatin replication in egg extract. Percentages of sperm peaks that are maintained after replication are indicated underneath.

Figure 4: ***H2AK119ub1 remodelling by egg factors is altered by sperm pre-treatment with a H2A deubiquitylase***

(**A**) Schematic representation of sperm treatment with oocyte extract containing USP21. (**B**) Left, Western blot of H2AK119ub1, H3K4me3, H3K9me3, H3K27me3 and histone H4 on untreated sperm, USP21 treated sperm and oocyte extract treated sperm. Right, signal ratio of H2AK119ub1 to H4 in untreated sperm, USP21 treated sperm, or oocyte extract treated sperm. *** $p<0.005$, **** $p<0.001$, ratio paired t test (n=6). Median is shown. (**C**) DNA fragments generated by MNase digestion of *Xenopus laevis* untreated sperm, oocyte control extract treated sperm, oocyte USP21 extract treated sperm, egg extract treated sperm and somatic cell. (**D**) Western blot analysis of H2AK119ub1 and histone H4 on sperm after treatment with control- or USP21- oocyte extract without (left) or with (right) subsequent replication in egg extract. (**E**) Heatmap of H2AK119ub1 and H3K4me3 signal (log(ChIP/Input)) in sperm after treatment with control- or USP21- oocyte extract without or with subsequent replication in egg extract. All genomic locations enriched for H2AK119ub1 (peaks) in replicated samples are represented. (**F-I**) DNAme and H2AK119ub1 signal (log(ChIP/Input)) on *Xenopus laevis* genome CpG island (F) and repeat element (H). Z-score of H2AK119ub1 enrichment on CpG island (G) and repeat element (I) in sperm, replicated sperm and replicated USP21 sperm. *** $p<0.005$, permutation test. Numbers of H2AK119ub1 peak overlapping the genomic feature are indicated for each cell type.

Figure 5: ***Sperm pre-treatment with a H2A deubiquitylase decreases developmental potential and leads to embryonic gene misregulation***

(**A**) Experimental design for the generation of haploid embryos from sperm or USP21 treated sperm. *Xenopus* illustrations © Natalya Zahn (2022) from Xenbase (www.xenbase.org RRID:SCR_003280). (**B**) Developmental progression to blastula, gastrula or swimming tadpole stage of haploid embryos derived from a USP21 or control oocyte extract treated sperm. Chi-squared test, * p-value<0.05. Median and SD values are shown. (**C**) MA-Plot showing as y-axis the log foldchange (Log2FC) of gene expression between control oocyte extract treated sperm *versus* untreated sperm (left) and between USP21 oocyte extract treated sperm derived embryo and control oocyte extract treated sperm (right). x-axis is the averaged gene expression across samples.

Figure 6: ***Genes sensitive to sperm deubiquitylase treatment are H2AK119ub1 target***

(**A**) Heatmap showing expression of differentially expressed gene in gastrulae derived from USP21 oocyte extract treated sperm *versus* that derived from control oocyte extract treated sperm. **(B)** Z-score of different H2AK119ub1 peaks categories

513 enrichment on TSS, enhancer, and gene body of USP21 sensitive genes. * p-
514 value<0.05; ** p-value < 0.01, permutation test. Number of H2AK119ub1 peak
515 overlapping the USP21 sensitive gene feature are indicated for each category. **(C)**
516 H2AK119ub1 and H3K4me3 signal on TSS +/- 5kB for all genes (black), USP21
517 sensitive genes (red) before and after sperm replication. *** p-value<0.001, Wilcoxon-
518 Mann-Whitney test on TSS+/1kb interval (shaded orange area). **(D)** Calibrated
519 H2AK119ub1 ChIP-seq signal on TSS +/- 5kB for all genes (black), USP21 sensitive
520 genes (red) before and after sperm replication. *** p-value<0.001, Wilcoxon-Mann-
521 Whitney test. **(E)** Z-score of USP21 sensitive gene enrichment on H2AK119ub1 peaks
522 gained (USP21 specific), lost (Control specific) or maintained (common) in replicated
523 USP21 treated sperm *versus* replicated control sperm. ***p-value<0.001, permutation
524 test. Number of USP21 sensitive gene overlapping each category is shown. **(F)**
525 Calibrated H2AK119ub1 ChIP-seq signal on TSS +/- 5kB for all genes (black), USP21
526 sensitive genes (red) before and after replication using a control oocyte extract treated
527 sperm or USP21 treated sperm. *** p-value<0.001, Wilcoxon-Mann-Whitney test.

528

529

530 **Figure 7:** ***Model of H2AK119ub1 epigenetic programming of sperm for embryonic***
531 ***development in Xenopus laevis***

532

533 **Supplemental Figure 1**: ***Quantification of Western blot data.***

534 **(A)** Ratio of fluorescence intensity detected by WB for H2AK119ub1/H2A (left)
535 H2AK119ub1/H4 (right) and H2A/H4 (middle). The same data as Fig.1G are plotted
536 with the addition of a solid line linking paired sample quantified in the same WB
537 experiment. **(B)** H2AK119ub1 fluorescence intensity detected by WB in untreated,
538 control oocyte extract treated sperm, USP21 extract treated sperm. The same data as
539 Fig.2E are plotted with the addition of a solid line linking paired sample quantified in
540 the same WB experiment.

541 **Supplemental Figure 2**: ***Pooling strategy for ChIP-seq replicates***

542 **(A)** Genome browser view of the log(ChIP/Input) for H2AK119ub1 around the *hoxa.L*
543 cluster on 3 sperm biological replicates. (**B**) Spearman correlation of sperm and
544 replicated sperm H2AK119ub1, H3K27me3 and H3K4me3 ChIP-seq replicates. (**C**)
545 (**D**) Heatmap illustrating the distribution of H2AK119ub1 and H3K4me3 in sperm and
546 replicated sperm replicates and in the corresponding pooled sample obtained by
547 subsampling. Log(ChIP/Input) signal is shown for TSS (C) and CpG (D), respectively.
548 (**E**) Fingerprint plot of Input, H3K4me3, H3K27me3, and H2AK119ub1 sperm ChIP
549 samples.

550 **Supplemental Figure 3**: ***Peak calling using RECOGNICER and SICER/MACS2.***

551 **(A)** Overlap of peaks called using RECOGNICER, SICER, and MACS2. Numbers in
552 red indicate RECOGNICER specific peaks *versus* those overlapping with those of
553 SICER and/or MACS2. Diagram scaling is based on RECOGNICER peaks. Blue and
554 green numbers correspond to the same comparison using SICER or MACS2 as the
555 reference set of peaks, respectively. (**B**) Heatmap of H2AK119ub1, H3K27me3,

556 H3K4me3 signal (log(ChIP/Input)) for RECOGNICER, SICER, and MACS2 set of
557 peaks. (**C**) Comparison of Z-scores obtained from permutation test using set of peaks
558 based on peaks set on peak calling using RECOGNICER (top row, corresponding to
559 data presented in Fig. 2K, Fig. 2M, Fig. 3H and Suppl Fig. 10G) or SICER (bottom
560 row). (**D**) Genomic distribution of sperm H2AK119ub1 peaks according to overlap with
561 H3K4me3 and/or H3K27me3 peaks when calling peak using RECOGNICER (top,
562 corresponding to data presented in Fig. 1I) or SICER (bottom) **(E)** Z-score indicating
563 enrichment of different H2AK119ub1 peaks categories on TSS +/-5kb, enhancer, and
564 gene body of USP21 sensitive genes. Top row is using RECOGNICER (already shown
565 in Fig. 3E) while bottom row is using SICER for H2AK119ub1 peak calling.

566 **Supplemental Figure 4**: ***H2AK119ub1 is mostly associated with nucleosomes while***
567 ***H3K4me3/H3K27me3 are mostly associated with sub-nucleosomes in Xenopus laevis***
568 ***sperm.*** (**A**) Schematic representation of *Xenopus laevis* chromatin remodelling from
569 nucleosomes to a mixture of nucleosomes and sub-nucleosomes during spermiogenesis.
570 (**B**) Fragment size distribution obtained after paired-end sequencing of chromatin
571 immunoprecipitated with antibodies against H2AK119ub1 (pink) in sperm and
572 spermatid, and against H3K4me3 (green) and H3K27me3 (yellow) in sperm. Matching
573 Input fraction are shown in grey.

574 **Supplemental Figure 5**: ***Sperm H2AK119ub1 fate following exposure to egg factors***

575 (**A**) Heatmap of H2AK119ub1 (pink), H3K4me3 (green), and H3K27me3 (yellow)
576 log(ChIP/Input) signal ratio on genes TSS from spermatid, sperm prior and after egg
577 extract treatment, and gastrula stage 12 embryo. (**B**) Scaled Venn diagram of
578 H2AK119ub1, H3K4me3 or overlapping H2AK119ub1/H3K4me3 peaks in spermatid,
579 sperm, and sperm exposed to egg factors. Percentage of peaks that are maintained at
580 each developmental transition are indicated underneath. (**C**) Top: boxplot showing
581 calibrated H2AK119ub1 on H2AK119ub1/H3K4me3 peaks lost (375), maintained
582 (5222) or gained (10442) following exposure to egg factors (top). Bottom: peak size
583 (blue dots) as well as H2A (red dots) in each peak category. **(D)** Genomic distribution
584 of sperm peaks before or after replication, as well as the subset of peaks lost, maintained,
585 or gained during replication**.**

586 **Supplemental Figure 6**: ***H2AK119ub1 distribution from spermiogenesis to late***
587 ***embryogenesis.***

588 (**A**) Pearson correlation of H2AK119ub1 ChIP in spermatid, sperm, sperm replicated
589 in egg extract, blastulae at ZGA, early gastrula, and late neurula. (**B**) (**C**) Heatmap of
590 H2AK119ub1 log(ChIP/Input) signal for TSSs (B) and CpG islands (C) in spermatid,
591 sperm, sperm replicated in egg extract, blastulae at ZGA, early gastrula, and late
592 neurula. **(D)** Metaplot analysis of H2AK119ub1 log(ChIP/Input) signal for TSSs of all
593 genes (black) or USP21 sensitive genes (red) in spermatid, sperm, sperm replicated in
594 egg extract, blastulae at ZGA, early gastrula, and late neurula. *** p-value<0.001,
595 Wilcoxon-Mann-Whitney test on TSS+/1kb interval (shaded orange area).

596 **Supplemental Figure 7**: ***Effect of oocyte extract treatment on sperm chromatin***

597 **(A)** Quantitation of H3K4me3, H3K9me3 and H3K27me3 to H4 WB signal ratio in
598 untreated sperm, USP21 treated sperm or control oocyte extract treated sperm, **(B)**
599 Capillary electrophoresis analysis of DNA fragments obtained following MNAse
600 digestion of somatic cell (yellow), egg extract treated sperm (dark blue), sperm (blue),

601 control oocyte extract treated sperm (cyan), and USP21 extract treated sperm (red). (**C**)
602 Fragment size distribution obtained after paired-end sequencing of DNA fragments
603 obtained following MNase digestion of sperm (top row), control oocyte extract treated
604 sperm (middle row) or USP21 treated sperm (bottom row) without (left column) or with
605 (right column) subsequent incubation in egg extract. (**D**)(**E**) Heatmap of H2AK119ub1
606 and H3K4me3 log(ChIP/Input) signal for TSSs (D) and CpG islands (E) in sperm and
607 sperm treated with control oocyte extract.

608 **Supplemental Figure 8***: Fate of sperm H2AK119ub1 and H3K4me3 following*
609 ***exposure to egg factors.***

610 (**A**) Experimental design for monitoring modified histones fate from control oocyte
611 extract or USP21 treated sperm. **(B)** Heatmap of H2AK119ub1 (pink), H3K4me3
612 (green) and H3K27me3 (yellow) log(ChIP/Input) signal in spermatid, control oocyte
613 extract- and USP21- treated sperm prior and after egg extract treatment, and gastrula
614 stage 12 embryo. Heatmap includes the same genomic location as in **Fig. 2B**. **(C)**
615 Heatmap of H2AK119ub1 and H3K4me3 signal log(ChIP/Input) in sperm after
616 treatment with control oocyte extract or USP21 oocyte extract without or with
617 subsequent replication in egg extract. All genomic locations enriched for H3K4me3
618 (peaks) in replicated samples are shown. (**D**) Transcription factor motifs enriched in
619 peaks that are lost, maintained, or gained upon replication of control versus USP21
620 treated sperm (clusters from Figure 4E).

621 **Supplemental Figure 9***: H2AK119ub1 is enriched on repeat elements of the genome*
622 ***following exposure of USP21 treated sperm to egg factors.***

623 (**A**) Metaplot analysis of H2AK119ub1 log(ChIP/Input) signal on all CpG islands
624 (10630 elements) and all repeat elements of the genome (313338 elements). * p-
625 value<0.005, Wilcoxon-Mann-Whitney test is indicated with an asterisk in black
626 (replicated control sperm *versus* replicated USP21 sperm), blue (replicated control
627 *versus* control sperm) or red (replicated USP21 sperm *versus* control sperm). (**B**) same
628 analysis as in (**A**) but splitting repeat elements according to subtypes.

629

630 **Supplemental Figure 10***: Genes misexpressed in embryos upon H2AK119ub1*
631 ***removal by deubiquitylases are associated with H2AK119ub1 in sperm.***

632 **(A)** Principal Component analysis of replicate RNA-seq samples used in this study
633 (USP21, USP21 extract treated sperm derived gastrulae; Control, control oocyte extract
634 treated sperm derived gastrulae; Untreated, untreated sperm derived gastrulae). **(B)**
635 Hierarchical clustering of replicate samples used in this analysis. **(C)** Heatmap
636 depicting expression of USP21 sensitive genes in replicates from USP21 extract treated
637 sperm derived gastrulae, control extract treated sperm derived gastrulae, as well as
638 gastrulae derived from untreated sperm. **(D)** Heatmap of gene expression in single
639 haploid gastrula derived from control- or USP21-treated sperm. Expression is shown
640 for the USP21 sensitive gene set identified on embryos pool (**Fig. 3D**). **(E)** USP21
641 sensitive gene set expression during early *Xenopus laevis* embryo development (data
642 from[33]). Expression is shown for oocyte, egg, blastulae (stage 8-9), gastrulae (stage 10-
643 12), neurula (stage 15-20), as well as early to late tailbud (stage 25-40) are indicated.
644 The right-hand side panel shows the expression of USP21 sensitive gene in gastrulae
645 derived from control- and USP21-treated sperm. **(F)** Violin plot of gene expression in

egg (log of normalised gene count) for all genes (black), USP21 sensitive genes (red), maternal genes (cyan), maternal and zygotic genes (green) and zygotic only gene (orange). USP21 sensitive genes are enriched for genes with maternal and zygotic expression in *Xenopus laevis*. The table below indicates p-Value resulting from a permutation test to evaluate enrichment of USP21 sensitive gene for either maternal-zygotic (MZ) or zygotic only (Z) genes. MZ and Z dataset taken from[34,35]. **(G)** Z-Score of H2AK119ub1 peak enrichment on TSS, enhancer, and gene body of USP21 sensitive genes. *p-value<0.05; permutation test. **(H)** Left, Heatmap representing H2AK119ub1 dynamics of each ChromHMM type in spermatid, sperm, replicated sperm, and gastrulae embryos. Color intensity represents H2AK119ub1 signal for a given state and cell type. Right, Z-score indicating enrichment for USP21 sensitive genes in genomic regions associated with the different chromHMM states. *p-value<0.05; **p-value < 0.01, ***p-value<0.001, permutation test. **(I)** Z-score of different H2AK119ub1 peaks sets enrichment on TSS, enhancer, and gene body of USP21 sensitive genes. Z-score are shown for sets corresponding to H2AK119ub1 peaks that are lost, maintained or gained following incubation of sperm in egg extract as well as for the subset of maintained H2AK119ub1 overlapping H3K4me3 peaks. *p-value<0.05; **p-value < 0.01, ***p-value<0.001, permutation test. **(J)** Experimental scheme used in Chen *et al.*, Nature genetics, 2021[19]. (**K**) Left, Heatmap representing H2AK119ub1 dynamics of each ChromHMM type in mouse embryos and gametes based on data generated[19]. Color intensity represents H2AK119ub1 percentage for a given state and cell type. Right, Z-score indicating enrichment for BAP1 sensitive genes identified in[19] in genomic regions associated with the different chromHMM states. *p-value<0.05; **p-value < 0.01, ***p-value<0.001, permutation test. (**L**) Calibrated H2AK119ub1 ChIP signal on TSS +/- 5kb for all genes (black), USP21 sensitive genes (red), maternal genes (cyan), maternal zygotic genes (green) and zygotic genes (orange) before and after sperm replication. *** p-value<0.001, Wilcoxon-Mann-Whitney test.

<u>Supplemental Table 1</u>*: Histone PTMs ChIP-seq*

<u>Supplemental Table 2</u>: *Gene Ontology and TF motif analysis related to Fig.2*

<u>Supplemental Table 3</u>: *Gene Ontology related to Supplemental Fig.8*

<u>Supplemental Table 4</u>: *Control- and epigenetically edited- sperm derived embryos RNA-seq data*

<u>Supplemental Table 5</u>: *Repeat element analysis*

<u>Supplemental Table 6</u>: *Extended Permutation test data*

683 **MATERIALS AND METHODS**

684 **Contact for Reagent and Resource Sharing.** Further information and requests for
685 resources and reagents should be directed to and will be fulfilled by the Lead Contact,
686 Dr J. Jullien (jerome.jullien@inserm.fr).

687 **Experimental Model and Subject Details.** Mature *Xenopus laevis* females were
688 obtained from Tefor Paris-saclays (151 Rte de la Rotonde, 91400 Saclay, France,
689 https://tefor.net/tefor-paris-saclay-nos-equipes/tefor-paris-saclay-aqua/). Our work
690 with Xenopus complied with all relevant ethical regulations for animal testing and
691 research. Work with frog was covered under the licence #202212131604754/APAFIS
692 39794V2 and frog husbandry and all experiments were performed according to the
693 relevant regulatory standards. Animals were kept in a recirculating system (ALS,
694 https://www.aquariumlocationservices.fr/professionnels-elevages-aquatique-
695 aquariophilie/) at a density of one adult/3l, with ~10% water change per day. Water
696 was sequentially filtered with mechanical pad sump filter, nitrifying bacteria filter, and
697 UV sterilized. Water quality parameters were as follow: temperature 17-22°C; PH 6-8.
698 Photoperiod was set to 12h ON/12h OFF. Frogs are fed twice per week with NEO
699 MARIN coul 4 - X4 - S20 (Le Gouessant, https://www.legouessant.com/).
700 Unconsumed food was removed 30 min after the start of feeding.

701 **Oocyte extract.** Fresh ovaries were manually dissociated in 15-25 oocytes clumps. 3-
702 5 mL of dissociated ovary fragments were transferred into 12.5 mL 1X Modified
703 Barth's Saline (MBS, 88 mM NaCl, 1 mM KCl, 10 mM Hepes, 2.4 mM NaHCO3, 1.7
704 mM MgSO4, 1.3 mM Ca(NO3)2, 0.8 mM CaCl2) supplemented with 250 µL of 5
705 mg/mL Liberase (Roche, 05 401 127 001) and incubated for 2h30-3h at room
706 temperature (RT) with gentle rocking. Defolliculated oocytes were washed three times
707 with 1X MBS and healthy stage 5-6 oocytes manually sorted. Oocytes were then
708 injected in the vegetal pole with 25 ng of USP21-NLS-HA mRNA, or control GFP
709 mRNA and incubated for 3 days at 18°C in 1X MBS, renewing medium and discarding
710 dead cells every day. ~500-1000 oocytes were collected in an Eppendorf tube on ice,
711 the excess 1X MBS discarded and replaced with 1X MBS supplemented with Protease
712 Inhibitor Cocktail (Sigma, P2714-1BTL). The oocytes were then stacked up by
713 centrifugation at 100 g for 1 min at RT and excess medium carefully discarded. Oocytes
714 were then thoroughly vortexed and centrifuged at 21 000g for 10 min at 4°C. The clear
715 intermediate phase between yolk (top) and pigment (bottom) was retrieved. The
716 collected fraction was further cleared by an additional centrifugation at 21 000 g for 10
717 min at 4°C. The oocyte extract was then aliquoted and stored at -80°C.

718 **Oocyte extract treatment.** Permeabilized sperm stored in SSB at -80°C were thawed,
719 washed with two volumes of ice cold 1X PBS and centrifuged at 800 g for 8 min at 4°C.
720 2M sperm in 1X PBS were centrifuged at 21000 g for 1 min at 4°C. The supernatant
721 was discarded, and the pelleted sperm resuspended in 10 µL of oocyte extract on ice.
722 The sperm incubated in the oocyte extract for 20-40 min at 23°C on a heating block.
723 Treatment was stopped by addition of 90 µL of ice cold 1X PBS and centrifugation at
724 21000 g for 1 min at 4°C. The supernatant discarded and the remaining pellets
725 resuspended in SSB for -80°C long term storage.

726 **Egg extract treatment.** Interphasic extracts were generated as previously
727 described[45] .For the quantification of DNA replication in individual nuclei in egg
728 extract, 33 µM rhodamine dUTP (Roche, 11534378910) was added at the indicated

729 times (20, 40, 60, 80 mins after incubation) for 5 min as indicated, and the reaction was
730 stopped with 1X PBS and fixed in 4% paraformaldehyde. The reaction was spun
731 through a 30 % sucrose cushion in PBS. The sperm cells were rinsed twice in 1X PBS
732 for 10 min and mounted in Vectashield mounting medium with DAPI (Vector
733 laboratories, H-1200). Counting of rhodamine positive cells were performed on an
734 epifluorescence microscope.

735 **Protein extraction and Western Blot analysis**. Sperm samples stored in SSB were
736 washed in 1X PBS and 1M sperm pellets were resuspended in 30 µL 2X Blue Eye (600
737 mM NaCl, 1 % Triton X100, 0.5 % Na-Deoxycholate, 4 % Sodium Dodecyl Sulfate,
738 20 % Glycerol, 0.0004 % Bromophenol blue, 175 mM Tris-HCl, 10 % Betamercapto
739 ethanol), boiled at 96°C for 5 min and centrifuged at 21000g for 5 min at 4°C. The
740 supernatant was transferred to a new tube and directly use for analysis or stored at -
741 20°C. 4-20 % mini-PROTEAN® TGX (Biorad, #4561094) were loaded with 10 µL of
742 sample and western blot analysis were performed according to standard protocols. For
743 blotting nitrocellulose membranes, a semi-dry transfer was used (Biorad, Trans-Blot®
744 SD Semi-Dry Transfer Cell) 30-40 min at 25V. The following primary antibodies were
745 used: anti-H2A (1:2500, Cell Signalling, 3636), anti-H2AK119ub1 (1:2500, Cell
746 Signalling, 8240), anti-H3K4me3 (1:2500, Abcam, ab8580), anti H3K9me3 (1:2500,
747 Abcam, ab8898), anti-H3K27me3(1:2500, Cell Signalling, 9735S), anti-H4 (1:2500,
748 Abcam, ab31830) and anti-HA (1:2500, Sigma, H9658). Membranes were incubated
749 with primary antibodies 2 h at RT or overnight (ON) at 4 °C. Secondary antibody are
750 anti-rabbit (1:25000, ThermoFisher, A21076), anti-mouse IgG Alexa Fluor 680
751 (1:25000, ThermoFisher, A21058), Goat anti-rabbit Alexa 800 (1:25,000,
752 ThermoFisher, A32735), or IRDye 800CW Goat Anti-Mouse IgG (H+L) (LI-COR,
753 926-32210) were used. The membranes were imaged either on a ChemiDoc MP
754 Imaging System (Biorad) or an Odyssey scanner (LI-COR).

755 **Sperm Chromatin Immunoprecipitation (ChIP).** Chromatin fractionation and
756 chromatin immunoprecipitation (ChIP) were performed as described before[10,44] with
757 slight modifications. 80 µL of Magnetic beads (M280 Sheep anti-rabbit IgG, Invitrogen,
758 #11204D) were used per reaction and all wash steps were carried out with a magnet.
759 Beads were washed with 1 mL of TE pH 8.0, lysis buffer (LB)(1:1 mixture of Buffer 1
760 and MNase buffer, see below), and incubated in 1 mL of LB with 100 µL of 10 mg/mL
761 BSA at 4°C for 30 min ("pre-blocking"). Pre-blocked beads were washed with 1 mL of
762 LB twice and resuspend in 80 µL of LB. Half of beads were incubated with antibody
763 overnight and leftovers were stored in 4°C for "pre-clear chromatin" step. For ChIP,
764 the following antibodies were used: anti-H3K4me3 (Abcam, ab8580), anti-
765 H2AK119ub1 (Cell Signaling, 8240). One million digitonin permeabilised sperm
766 nuclei or egg extract treated sperm nuclei were resuspended in 50 µL of Buffer 1 (0.3
767 M Sucrose, 15 mM Tris pH 7.5, 60 mM KCl, 15 mM NaCl, 5 mM MgCl2, 0.1 mM
768 EGTA, 0.5 mM DTT) containing 0.125 ng H2AK119ub biotinyltated nucleosome
769 (Epicypher #16-0020), followed by addition of 50 µL of Buffer 1 with detergent (Buffer
770 1 including 0.5 % NP40 and 1 % NaDOC). Samples were incubated for 10 min on ice.
771 100 µL of MNase buffer (0.3 M Sucrose, 85 mM Tris, 3 mM $MgCl_2$, 2 mM $CaCl_2$, 2.5
772 U of micrococcal nuclease: Roche 10107921001) was added in to each tube (0.5 million
773 of cells per tube). Tubes were incubated at 37°C for 30 min in pre-warmed water bath.
774 Reaction was stopped by adding 2 µL of 0.5 M EDTA pH 8.0 in the same order as
775 started. Tubes were vortexed and placed on ice for at least 5 min. Supernatant and pellet
776 were separated by centrifugation at 13000 rpm for 10 min at room temperature. Beads

777 (stored at 4C for pre-clear chromatin) were washed with 1 mL of LB twice. Supernatant
778 and EDTA-free Protease Inhibitor Cocktail were added into the beads and rotating on
779 the wheel at 4°C for 60 min. 10% of volume of pre-cleared chromatin was taken as
780 "Input" and stored at 4°C. Antibody conjugated beads were washed with 1 mL of LB
781 twice. Pre-cleared chromatin was added to washed beads and incubated at 4°C for 6 h.
782 After incubation, beads were washed with 1 mL of Washing buffer A (50 mM Tris-HCl
783 pH 7.5, 10 mM EDTA and 75 mM NaCl) on the wheel at 4C for 5 min and buffer was
784 discarded carefully. Subsequently, beads were washed wish 1 ml of Washing buffer B
785 (50 mM Tris-HCl pH 7.5, 10 mM EDTA and 125 mM NaCl) and buffer was discarded
786 carefully. Another 1 mL of Washing buffer B was added and transferred to 1.5 mL
787 Protein lo-bind tubes (Eppendorf, 0030108116) with beads. Buffer was discarded
788 carefully. 150 µL of elution buffer (1:9 mixture of 10 % SDS and TE) was added. Tubes
789 were placed at 25°C on the Eppendorf thermomixer and shaken at 800 rpm for 15 min.
790 Supernatant were taken and transferred to the new tube using magnetic stand. Another
791 150 µL of elution buffer was added and repeated this step (in total 300 µl). Input
792 samples were diluted to 300 µL total by adding TE. 2 µL of 2 mg/ml RNase A (heat-
793 inactivated or DNase-free) was added and incubated at 37°C for 30 min. 4 µL of 10
794 mg/ml Proteinase K was added and incubated at 55°C overnight. After incubation,
795 tubes were shortly spun. 300 µL of Phenol/chloroform were added and vortexed for 30
796 sec. Samples were centrifuged at 13000 rpm for 10 min at room temperature. 1 µL of
797 Glycogen, 1/10 volume of NaAcetate and 2 volumes of 100% EtOH were added and
798 vortexed. Tubes were stored on dry ice for 20-30 min. Once frozen, tubes were
799 centrifuged at 13000 rpm for 30 min at 4°C. Supernatant was discarded carefully and
800 500 µL of 70% EtOH was added. Tubes were centrifuged at 13000 rpm for 10 min at
801 4°C. Pellets were dried and suspended in 30 µL of ddH_2O.

802 **Embryo Chromatin Immunoprecipitation (ChIP).** Batches of 200 in vitro fertilized
803 embryos were fixed in 15 ml 1 % Paraformaldehyde in 1X MMR for 20min at room
804 temperature followed by 4 washes with 1X MMR. Embryos were split in two and
805 equilibrated at 4°C overnight in 500 µL HEG solution (50 mM HEPES-KOH pH 7.5,
806 1 mM EDTA, 20 % Glycerol), then excess buffer was discarded, and samples were
807 transferred to -80°C. For chromatin extraction embryos were resuspended in 700 µL of
808 sonication buffer (20 mM Tris-HCl pH 8.0, 70 mM KCl, 1 mM EDTA pH 8.0, 10%
809 Glycerol, 5 mM DTT, 0.125% NP40, 1X complete protease inhibitors) and
810 homogenized by pipetting up and down. 200 µL embryo extract were distributed in 1.5
811 mL tubes and sonicated in two sets of 15 min cycles (with 30 s on/off cycles). Sonicated
812 samples were centrifuged at 12000 rpm for 5 min at 4 °C a Supernatants were retrieved
813 and the centrifugation was repeated. Before ChIP, 180 µL (2x 10%) of the chromatin
814 extract was taken as an Input control and stored at -20°C. For each ChIP, 720 µL of
815 chromatin extract was mixed with 2 µL of anti-H2AK119ub1 antibodies (Cell
816 Signalling, 8240) and incubated overnight on a rotating wheel. The next day, 40 µL (20
817 µL per IP) of Magnetic beads (M280 Sheep anti-rabbit IgG, Invitrogen, #11204D) were
818 washed with 1X PBS using a magnet and incubated with 1mL of 1X PBS containing 1
819 mg/mL BSA for 2 h at 4°C on a rotating wheel. Blocking solution was discarded from
820 the beads using a magnet and beads were resuspended in 200 µL (100 µl per IP) of
821 incubation buffer (50 mM Tris-HCl pH 8, 100 mM NaCl, 2 mM EDTA, 1% NP40, 1
822 mM DTT, 1X Protease inhibitor). 100 µL of incubation buffer containing beads is
823 transferred to chromatin/antibody mix and incubated for 4 h at 4°C. Samples were
824 washed with Buffer 1 (50 mM Tris-HCl pH 8, 100 mM NaCl, 2 mM EDTA, 1 mM
825 DTT, 1 % NP40, 0.1 % sodium deoxycholate, 1X complete protease inhibitors) for 5

826 min at 4°C on rotating wheel. Using a magnet, supernatant was discarded and beads
827 subsequently washed with Buffer 2 (50 mM Tris-HCl pH 8, 500 mM NaCl, 2 mM
828 EDTA, 1 mM DTT, 1 % NP40, 0.1 % sodium deoxycholate, 1X complete protease
829 inhibitors), Buffer 3 (50 mM Tris-HCl pH 8, 100 mM NaCl, 250 mM LiCl, 2 mM
830 EDTA, 1 mM DTT, 1 % NP40, 0.1 % sodium deoxycholate, 1X complete protease
831 inhibitors), Buffer 1 after which immunoprecipitated chromatin was eluted using 400
832 µL (310 µL for Input fraction) of Elution buffer (0.1 M NaHCO3, 1 % SDS) overnight
833 at 65°C. The next day, 4 µL of 20 mg/mL RNAse A was added to the chromatin solution
834 and incubated for 2 h at 37°C. After incubation, tubes were shortly spun. 300 µL of
835 Phenol/chloroform were added and vortexed for 30 sec. Samples were centrifuged at
836 13,000 rpm for 10 min at room temperature. 1 ul of Glycogen, 1/10 volume of
837 NaAcetate and 2 volumes of 100% EtOH were added and vortexed. Tubes were stored
838 on dry ice for 20-30 min. Once frozen, tubes were centrifuged at 13,000 rpm for 30 min
839 at 4C. Supernatant was discarded carefully and 500 µL of 70% EtOH was added. Tubes
840 were centrifuged at 13,000 rpm for 10 min at 4C. Pellets were dried and suspended in
841 30 μl of ddH2O.

842 ***Xenopus* sperm collection *Xenopus* sperm collection.** *Xenopus* sperm collection was
843 performed as described before[10,44]. For each round of sperm purification, testes from
844 six adult *Xenopus laevis* males were isolated and manually cleaned from blood vessels
845 and fat bodies in 1X Marc's Modified Ringers (MMR, 100 mM NaCl, 2 mM KCl, 1
846 mM $MgSO_4$, 2 mM $CaCl_2$, 3 mM HEPES, pH 7.4) using forceps and paper tissues.
847 Subsequently, testes were torn into small pieces with forceps and homogenized with 2–
848 3 strokes of a Dounce homogenizer (one testis at a time). The cell suspension was then
849 filtered to remove tissue debris and cell clumps using a 60 µm Mesh (CellTrics, cat.
850 04-0042-2317) and spun down at 800 rcf, 4°C, for 20 min. Supernatant was discarded
851 and the cell pellet was resuspended in 12 mL of 1 × MMR. If any red blood cells were
852 visible at the bottom of the pellet (as a result of incomplete removal of blood vessels),
853 only the uncontaminated part of the pellet was recovered, taking extreme care not to
854 disturb the red blood cells. Subsequently, step gradients of iodixanol (Optiprep; Sigma,
855 D1556; 60% iodixanol in water) in 1X MMR final were manually prepared in pre-
856 chilled 14 mL ultra- clear centrifuge tubes (Beckman Coulter, #344060) in the
857 following order from the bottom to the top of the tube: 4 mL of 30 % iodixanol, 1 mL
858 of 20 % iodixanol, 5 mL of 12 % iodixanol (all in 1 × MMR), and 2 mL of cell
859 suspension in 1X MMR on top. Gradients were spun down in a pre-chilled SW40Ti
860 rotor at 7500 rpm (10,000g), 4°C, for 15 min, deceleration without brake (Beckman
861 Coulter Ultracentrifuge, Optima L-100XP). The pelleted fraction, containing mature
862 sperm, was collected. Collected fractions were diluted six times with 1X MMR and
863 collected by spinning first at 805 rcf, 4°C, for 20 min and then at 3220 rcf, 4°C, for 20
864 min to pellet remaining cells. Pelleted cells were subsequently permeabilized with
865 Digitonin (10 mg/mL as a final concentration, Sigma, D141) for 5 min at room
866 temperature as detailed before (Smith et al., 2006).

867 **Library preparation and sequencing.** ChIP samples were subjected to ChIP-seq
868 library preparation using QIAseq Ultralow Input Lib UDI-A Kit (Qiagen, 180497) and
869 Agencourt AMPure XP beads (Beckman coulter, A63881). Samples pre- and post-
870 library protocol were analyzed on a LabChip GX (PerkinElmer) using DNA 1KHS and
871 1K Assay LabChIP, respectively. Libraries were quantitated using NEBNext Library
872 Quant Kit (NEB, E7630,). For RNA sequencing, RNAs were purified using Qiagen
873 RNeasy Mini Kit (#74004) and used to generate cDNA sequencing libraries using an
874 Illumina TruSeq Kit (#RS-122-2001), according to the manufacturer's specifications.

875 Paired-end sequencing was carried out either on a NOVA-seq 6000 or HiSeq 1500
876 sequencer (Illumina).
877

878 **RNA-Seq analysis.** Adapters were trimmed and low-quality reads filtered using
879 cutadapt (v1.18)[46]. Sample quality was confirmed with fastqc (v0.11.8)[47]. fastq were
880 aligned to *Xenopus laevis* genome (v9.2) using STAR aligner (v2.7.3.a)[48]. Count table
881 was generated using HTSeq-count (v0.12.3)[49] and exon as genes reference. MultiQC
882 (v1.9)[50] summarized data pre-processing. Differential gene expression analysis of the
883 count table was performed on R (v3.6)[51] using DESeq2tools[52]. Details of the pipeline
884 used can be found at https://gitlab.univ-nantes.fr/E114424Z/BulkRNAseq. Gene
885 ontology analysis were carried out with gprofiler[53] using human orthologs of *Xenopus*
886 *laevis* genes recovered from Xenbase (https://www.xenbase.org/xenbase/static-
887 xenbase/ftpDatafiles.jsp)[54]. *Xenopus laevis* development RNA-seq data were from
888 published dataset GSE73430.

889

890 **ChIP-Seq analysis.** Adapters were trimmed and low-quality reads filtered using
891 cutadapt (v1.18)[46]. Sample quality was confirmed with fastqc (v0.11.9)[47]. Alignment
892 was performed with bwa mem[55] against *Xenopus laevis* (v9.2) or against a *Xenopus*
893 *laevis* (v9.2) - 601DNA hybrid genome generated with bwa index (v0.7.17-r1188).
894 Reads extraction and analysis was performed with samtools view and samtools flagstat
895 (v1.12)[56]. ChIP-Seq sample quality was assessed by Deeptools (v3.5.1)[57] using
896 plotFingerprint function and bamPEFragmentSize. Replicates quality was visualised
897 with plotCorrelation using spearman correlation after genome fragmentation into bins
898 of 10Kb. PCR duplicates were marked by Picard tools using MarkDuplicates command
899 (https://broadinstitute.github.io/picard) and then removed with samtools view -F 0x400.
900 Replicates were pooled by subsampling the same amount of reads per replicates using
901 sambamba (v0.8.1)[58] and samtools view (-s option). Peak calling was processed with
902 MACS2 (https://github.com/macs3-project/MACS)[59] (-q 0.01 --nomodel --extsize 147
903 --gsize=2.6e9) for H3K4me3, with MACS2 broad option for H3K27me3 (--broad --
904 broad-cutoff 0.1 -q 0.01 --nomodel --extsize 147 --gsize=2.6e9) and RECOGNICER[24]
905 (qvalue 0.001) /MACS2 (--broad --broad-cutoff 0.1 -q 0.01 --nomodel --extsize 147)
906 for H2AK119ub1. SICER peak calling was performed using the following parameters
907 -s XL -w 200 -rt 1 -f 150 -egf 0.74 -fdr 0.001 -g 600 -e 1000. Peaks overlap was defined
908 using bedtools intersect having at least 1 bp of overlap between peaks. H2AK119ub1
909 signal was calibrated using reads mapping to the 601DNA and corresponding to the
910 fully ubiquitylated H2AK119 nucleosome spiked-in in samples prior to ChIP (see ChIP
911 M&M section). To evaluate difference in modifed histone ChIP-seq signal around the
912 TSS of gene sets, Wilcoxon Mann-Whitney test was performed on the +/-1 kb window
913 around the TSSs. ChIPSeeker[60] and ChIPPeakAnno[61,62] were used to annotate peaks on
914 R[51]. The RegioneR[63] package was used to perform peaks permutation and assess
915 enrichment on USP21 sensitive gene features (*i.e.* TSS, enhancer, or gene body)
916 compared to a random set of genes (using 10000 iterations of the resampleRegions
917 function, , for Fig.3E, .3H, .S3C two right panels, .S3E, .S10G, .S10I) and to assess
918 peak enrichment on genomic features (using 1000 iterations of the randomizeRegions
919 function, for Fig 1G, 2K, 2M, S3C two left panels, S10H, S10K). Log10 (ChIP/Input)
920 was computed using Deeptools with BamCompare using 50bp binsize. Heatmap and
921 TSS plot were produced with computeMatrix and plotHeatmap or plotProfile. IGV was
922 used for peaks and log10(ChIP/Input) signal visualisation. Heatmap were produced

923 with computeMatrix using 50bp binsize +/-5kb of TSS or peak center. Heatmaps were
924 generated with plotHeatmap function using unsupervised clustering (--hclust option),
925 and metaplot using plotProfile function. IGV[64] was used to visualize output signal
926 tracks. Bedtools getfasta[65] was used to extract FASTA sequences corresponding to
927 peaks from a selected heatmap cluster. To identify transcription factors motif in the
928 selected peak set, Homer[66] was then used with the findMotifs.pl function and all other
929 peaks of the heatmap as a background set. CpG islands and repeats elements were
930 recovered from UCSC genome annotation database
931 (https://hgdownload.soe.ucsc.edu/goldenPath/xenLae2/database/). For genome
932 partitioning approach, chromHMM model was initialized using BinarizeBam on ChIP
933 and Input sample file, using binsize of 150bp (-b 150). The model was trained using a
934 random initiation (-init random), over binsize of 150bp (-b 150) and a maximum of
935 5000 iterations (-r 5000). SNPsplit was used for reads assignment to paternal and
936 maternal copies as described in[19].

937

938 **Data Availability.** The *Xenopus laevis* ChIP-seq and RNA-seq data generated for this
939 study will be referenced as PRJEB56442 at the European Genome-phenome Archive
940 (EGA). Additional dataset used are from GSE73430 (Xenopus embryo RNA-seq),
941 GSE125982 (sperm and replicated sperm H3K27me3 ChIP-seq), GSE126599
942 (Gastrulae H3K27me3, , and H3K4me3 ChIP-seq), and GSE75164 (sperm MBD-seq,
943 spermatid H3K27me3), and GSE153531 (H2AK119ub1Cut&Run mouse embryos and
944 gametes).

945 **Code Availability.** All scripts used for these analyses are available on Github
946 (https://github.com/FCValentin/H2AubPaper).

947

948 **AUTHORS CONTRIBUTION**

949 Conceptualization: JJ; Methodology: JJ, VF-C, FB, LP; Validation: JJ, VF-C, FB;
950 Formal analysis: VF-C, FB, MO, MG, VC; Investigation: JJ, VF-C, FB, NM, CF, JP,
951 RG, MO, BH, KP, JGA; Writing original draft: JJ; Writing review and editing: JJ, FB,
952 VFC. Visualisation: FB, VF-C; Supervision: JJ; Project administration: JJ; Funding
953 acquisition: JJ.

954

955 **COMPETING INTERESTS**

956 The authors declare no competing interests

957

958 **ACKOWLEDGEMENTS**

959 J.J group is funded by ANR-21-CE13-0031-01 grant from the Agence Nationale de la
960 Recherche and a Connect Talent grant from Ville de Nantes and Region pays de la
961 Loire. M.O is funded by a postdoctoral fellowship from the Japan Society for the
962 Promotion of Science (JSPS). R.G was supported for this work by a Career
963 Development Award grant (CDA00019/2019-C) form the Human Frontier Science

964 Program.. L.P group is supported by NIH award R24 OD031956. We would like to
965 acknowledge the support of Xenbase.
966
967
968 **REFERENCE**

969 1. Öst, A. *et al.* Paternal diet defines offspring chromatin state and
970 intergenerational obesity. *Cell* (2014) doi:10.1016/j.cell.2014.11.005.

971 2. Dias, B. G. & Ressler, K. J. Parental olfactory experience influences behavior
972 and neural structure in subsequent generations. *Nat. Neurosci.* (2014)
973 doi:10.1038/nn.3594.

974 3. Radford, E. J. *et al.* In utero undernourishment perturbs the adult sperm
975 methylome and is linked to metabolic disease transmission. *Science (80-.).*
976 **345**, 1–26 (2015).

977 4. Ben Maamar, M., Beck, D., Nilsson, E. E., Kubsad, D. & Skinner, M. K.
978 Epigenome-wide association study for glyphosate induced transgenerational
979 sperm DNA methylation and histone retention epigenetic biomarkers for
980 disease. *Epigenetics* **16**, (2021).

981 5. Lismer, A., Siklenka, K., Lafleur, C., Dumeaux, V. & Kimmins, S. Sperm
982 histone H3 lysine 4 trimethylation is altered in a genetic mouse model of
983 transgenerational epigenetic inheritance. *Nucleic Acids Res.* **48**, (2020).

984 6. U., B. *et al.* Repressive and active histone methylation mark distinct promoters
985 in human and mouse spermatozoa. *Nature Structural and Molecular Biology*
986 (2010).

987 7. Hammoud, S. S. *et al.* Distinctive chromatin in human sperm packages genes
988 for embryo development. *Nature* (2009) doi:10.1038/nature08162.

989 8. Wu, S. F., Zhang, H. & Cairns, B. R. Genes for embryo development are
990 packaged in blocks of multivalent chromatin in zebrafish sperm. *Genome Res.*
991 (2011) doi:10.1101/gr.113167.110.

992 9. Teperek, M. *et al.* Sperm is epigenetically programmed to regulate gene
993 transcription in embryos. *Genome Res.* **26**, (2016).

994 10. Oikawa, M. *et al.* Epigenetic homogeneity in histone methylation underlies
995 sperm programming for embryonic transcription. *Nat. Commun.* (2020)
996 doi:10.1038/s41467-020-17238-w.

997 11. Siklenka, K. *et al.* Disruption of histone methylation in developing sperm
998 impairs offspring health transgenerationally. *Science (80-.).* (2015)
999 doi:10.1126/science.aab2006.

1000 12. Murphy, P. J., Wu, S. F., James, C. R., Wike, C. L. & Cairns, B. R. Placeholder
1001 Nucleosomes Underlie Germline-to-Embryo DNA Methylation
1002 Reprogramming. *Cell* (2018) doi:10.1016/j.cell.2018.01.022.

1003 13. Blackledge, N. P. *et al.* Variant PRC1 complex-dependent H2A ubiquitylation
1004 drives PRC2 recruitment and polycomb domain formation. *Cell* **157**, (2014).

1005 14. Tamburri, S. *et al.* Histone H2AK119 Mono-Ubiquitination Is Essential for
1006 Polycomb-Mediated Transcriptional Repression. *Mol. Cell* **77**, (2020).

1007 15. Nakagawa, T. *et al.* Deubiquitylation of histone H2A activates transcriptional
1008 initiation via trans-histone cross-talk with H3K4 di- and trimethylation. *Genes*
1009 *Dev.* (2008) doi:10.1101/gad.1609708.

1010 16. Joo, H. Y. *et al.* Regulation of cell cycle progression and gene expression by
1011 H2A deubiquitination. *Nature* (2007) doi:10.1038/nature06256.

1012 17. Cao, J. & Yan, Q. Histone ubiquitination and deubiquitination in transcription,
1013 DNA damage response, and cancer. *Frontiers in Oncology* (2012)
1014 doi:10.3389/fonc.2012.00026.

1015 18. Chen, D., Dai, C. & Jiang, Y. Histone H2A and H2B Deubiquitinase in
1016 Developmental Disease and Cancer. *Cancer Transl. Med.* (2015)
1017 doi:10.4103/2395-3977.168578.

1018 19. Chen, Z., Djekidel, M. N. & Zhang, Y. Distinct dynamics and functions of
1019 H2AK119ub1 and H3K27me3 in mouse preimplantation embryos. *Nat. Genet.*
1020 **53**, (2021).

1021 20. Hickey, G. J. M. *et al.* Establishment of developmental gene silencing by
1022 ordered polycomb complex recruitment in early zebrafish embryos. *Elife* **11**,
1023 (2022).

1024 21. Conway, E. *et al.* BAP1 enhances Polycomb repression by counteracting
1025 widespread H2AK119ub1 deposition and chromatin condensation. *Mol. Cell*
1026 **81**, (2021).

1027 22. Albright, S. C., Nelson, P. P. & Garrard, W. T. Histone molar ratios among
1028 different electrophoretic forms of mono- and dinucleosomes. *J. Biol. Chem.*
1029 **254**, (1979).

1030 23. Matsui, S., Seon, B. K. & Sandberg, A. A. Disappearance of a structural
1031 chromatin protein A24 in mitosis: Implications for molecular basis of
1032 chromatin condensation. *Proc. Natl. Acad. Sci. U. S. A.* **76**, (1979).

1033 24. Zang, C., Wang, Y. & Peng, W. RECOGNICER: A coarse-graining approach
1034 for identifying broad domains from ChIP-seq data. *Quant. Biol.* **8**, (2020).

1035 25. Heard, E. & Disteche, C. M. Dosage compensation in mammals: Fine-tuning
1036 the expression of the X chromosome. *Genes and Development* vol. 20 (2006).

1037 26. Jullien, J. *et al.* Gene Resistance to Transcriptional Reprogramming following
1038 Nuclear Transfer Is Directly Mediated by Multiple Chromatin-Repressive
1039 Pathways. *Mol. Cell* **65**, (2017).

1040 27. Kuznetsov, J. N. *et al.* BAP1 regulates epigenetic switch from pluripotency to
1041 differentiation in developmental lineages giving rise to BAP1-mutant cancers.
1042 *Sci. Adv.* **5**, (2019).

1043 28. Jin, J. *et al.* The deubiquitinase USP21 maintains the stemness of mouse
1044 embryonic stem cells via stabilization of Nanog. *Nat. Commun.* (2016)

1045 doi:10.1038/ncomms13594.

1046 29. Gaggioli, V., Le Viet, B., Germe, T. & Hyrien, O. DNA topoisomerase IIα
1047 controls replication origin cluster licensing and firing time in Xenopus egg
1048 extracts. *Nucleic Acids Res.* **41**, (2013).

1049 30. Blackledge, N. P. & Klose, R. J. The molecular principles of gene regulation
1050 by Polycomb repressive complexes. *Nature Reviews Molecular Cell Biology*
1051 vol. 22 (2021).

1052 31. Zahn, N., Levin, M. & Adams, D. S. The zahn drawings: New illustrations of
1053 xenopus embryo and tadpole stages for studies of craniofacial development.
1054 *Dev.* **144**, (2017).

1055 32. Hörmanseder, E. *et al.* H3K4 Methylation-Dependent Memory of Somatic Cell
1056 Identity Inhibits Reprogramming and Development of Nuclear Transfer
1057 Embryos. *Cell Stem Cell* **21**, (2017).

1058 33. Session, A. M. *et al.* Genome evolution in the allotetraploid frog Xenopus
1059 laevis. *Nature* **538**, (2016).

1060 34. Chen, H. & Good, M. C. Imaging nascent transcription in wholemount
1061 vertebrate embryos to characterize zygotic genome activation. in *Methods in*
1062 *Enzymology* vol. 638 (2020).

1063 35. Chen, H., Einstein, L. C., Little, S. C. & Good, M. C. Spatiotemporal
1064 Patterning of Zygotic Genome Activation in a Model Vertebrate Embryo. *Dev.*
1065 *Cell* **49**, (2019).

1066 36. Tsuboi, M. *et al.* Ubiquitination-Independent Repression of PRC1 Targets
1067 during Neuronal Fate Restriction in the Developing Mouse Neocortex. *Dev.*
1068 *Cell* **47**, (2018).

1069 37. Żylicz, J. J. *et al.* The Implication of Early Chromatin Changes in X
1070 Chromosome Inactivation. *Cell* **176**, (2019).

1071 38. Mei, H. *et al.* H2AK119ub1 guides maternal inheritance and zygotic deposition
1072 of H3K27me3 in mouse embryos. *Nat. Genet.* **53**, (2021).

1073 39. Van Heeringen, S. J. *et al.* Principles of nucleation of h3k27 methylation
1074 during embryonic development. *Genome Res.* (2014)
1075 doi:10.1101/gr.159608.113.

1076 40. Akkers, R. C. *et al.* A Hierarchy of H3K4me3 and H3K27me3 Acquisition in
1077 Spatial Gene Regulation in Xenopus Embryos. *Dev. Cell* (2009)
1078 doi:10.1016/j.devcel.2009.08.005.

1079 41. Zhao, J. *et al.* RYBP/YAF2-PRC1 complexes and histone H1-dependent
1080 chromatin compaction mediate propagation of H2AK119ub1 during cell
1081 division. *Nat. Cell Biol.* **22**, (2020).

1082 42. Lismer, A. *et al.* Histone H3 lysine 4 trimethylation in sperm is transmitted to
1083 the embryo and associated with diet-induced phenotypes in the offspring. *Dev.*
1084 *Cell* **56**, (2021).

1085 43. Pepin, A. S., Lafleur, C., Lambrot, R., Dumeaux, V. & Kimmins, S. Sperm
1086 histone H3 lysine 4 tri-methylation serves as a metabolic sensor of paternal
1087 obesity and is associated with the inheritance of metabolic dysfunction. *Mol.*
1088 *Metab.* **59**, (2022).

1089 44. Teperek, M. *et al.* Sperm and spermatids contain different proteins and bind
1090 distinct egg factors. *Int. J. Mol. Sci.* **15**, (2014).

1091 45. Hannak, E. & Heald, R. Investigating mitotic spindle assembly and function in
1092 vitro using Xenopus laevis egg extracts. *Nat. Protoc.* **1**, (2006).

1093 46. Martin, M. Cutadapt removes adapter sequences from high-throughput
1094 sequencing reads. *EMBnet.journal* **17**, (2011).

1095 47. Andrews, S. & others. FastQC: a quality control tool for high throughput
1096 sequence data. 2010.
1097 *Https://Www.Bioinformatics.Babraham.Ac.Uk/Projects/Fastqc/* (2019).

1098 48. Dobin, A. *et al.* STAR: Ultrafast universal RNA-seq aligner. *Bioinformatics*
1099 **29**, (2013).

1100 49. Anders, S., Pyl, P. T. & Huber, W. HTSeq-A Python framework to work with
1101 high-throughput sequencing data. *Bioinformatics* **31**, (2015).

1102 50. Ewels, P., Magnusson, M., Lundin, S. & Käller, M. MultiQC: Summarize
1103 analysis results for multiple tools and samples in a single report. *Bioinformatics*
1104 **32**, (2016).

1105 51. Dessau, R. B. & Pipper, C. B. [''R"--project for statistical computing]. *Ugeskr.*
1106 *Laeger* **170**, (2008).

1107 52. Love, M. I., Huber, W. & Anders, S. Moderated estimation of fold change and
1108 dispersion for RNA-seq data with DESeq2. *Genome Biol.* **15**, (2014).

1109 53. Raudvere, U. *et al.* G:Profiler: A web server for functional enrichment analysis
1110 and conversions of gene lists (2019 update). *Nucleic Acids Res.* **47**, (2019).

1111 54. Fisher, M. *et al.* Xenbase: Key features and resources of the Xenopus model
1112 organism knowledgebase. *Genetics* **224**, (2023).

1113 55. Li, H. & Durbin, R. Fast and accurate short read alignment with Burrows-
1114 Wheeler transform. *Bioinformatics* **25**, (2009).

1115 56. Danecek, P. *et al.* Twelve years of SAMtools and BCFtools. *Gigascience* **10**,
1116 (2021).

1117 57. Ramírez, F. *et al.* deepTools2: a next generation web server for deep-
1118 sequencing data analysis. *Nucleic Acids Res.* **44**, (2016).

1119 58. Tarasov, A., Vilella, A. J., Cuppen, E., Nijman, I. J. & Prins, P. Sambamba:
1120 Fast processing of NGS alignment formats. *Bioinformatics* **31**, (2015).

1121 59. Zhang, Y. *et al.* Model-based analysis of ChIP-Seq (MACS). *Genome Biol.* **9**,
1122 (2008).

1123 60. Wang, Q. *et al.* Exploring Epigenomic Datasets by ChIPseeker. *Curr. Protoc.*
1124 **2**, (2022).

1125 61. Zhu, L. J. *et al.* ChIPpeakAnno: A Bioconductor package to annotate ChIP-seq
1126 and ChIP-chip data. *BMC Bioinformatics* **11**, (2010).

1127 62. Zhu, L. J. Integrative analysis of ChIP-chip and ChIP-seq dataset. *Methods*
1128 *Mol. Biol.* **1067**, (2013).

1129 63. Gel, B. *et al.* RegioneR: An R/Bioconductor package for the association
1130 analysis of genomic regions based on permutation tests. *Bioinformatics* **32**,
1131 (2016).

1132 64. Thorvaldsdóttir, H., Robinson, J. T. & Mesirov, J. P. Integrative Genomics
1133 Viewer (IGV): High-performance genomics data visualization and exploration.
1134 *Brief. Bioinform.* **14**, (2013).

1135 65. Quinlan, A. R. & Hall, I. M. BEDTools: A flexible suite of utilities for
1136 comparing genomic features. *Bioinformatics* **26**, (2010).

1137 66. Heinz, S. *et al.* Simple Combinations of Lineage-Determining Transcription
1138 Factors Prime cis-Regulatory Elements Required for Macrophage and B Cell
1139 Identities. *Mol. Cell* **38**, (2010).

1140 67. Flury,V. *et al.* Recycling of modified H2A-H2B provides short-term memory
1141 of chromatin states. *Cell* **186**, (2023).

1142

1143

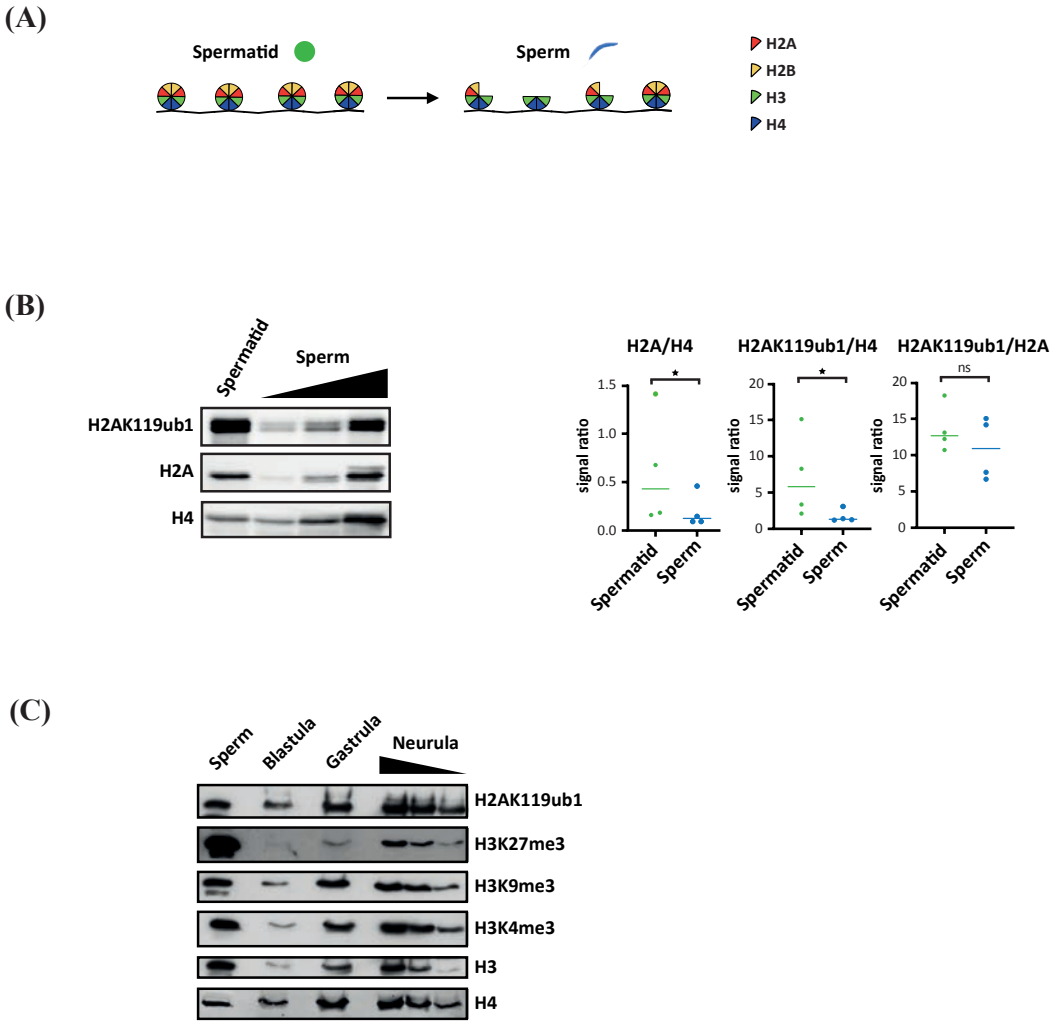
(A)
Spermatid
Sperm
H2A
H2B
H3
H4
(B)
Spermatid
Sperm
H2AK119ub1
H2A
H4
H2A/H4
H2AK119ub1/H4
H2AK119ub1/H2A
signal ratio
*
*
ns
Spermatid
Sperm
(C)
Sperm
Blastula
Gastrula
Neurula
H2AK119ub1
H3K27me3
H3K9me3
H3K4me3
H3
H4

FIGURE 1

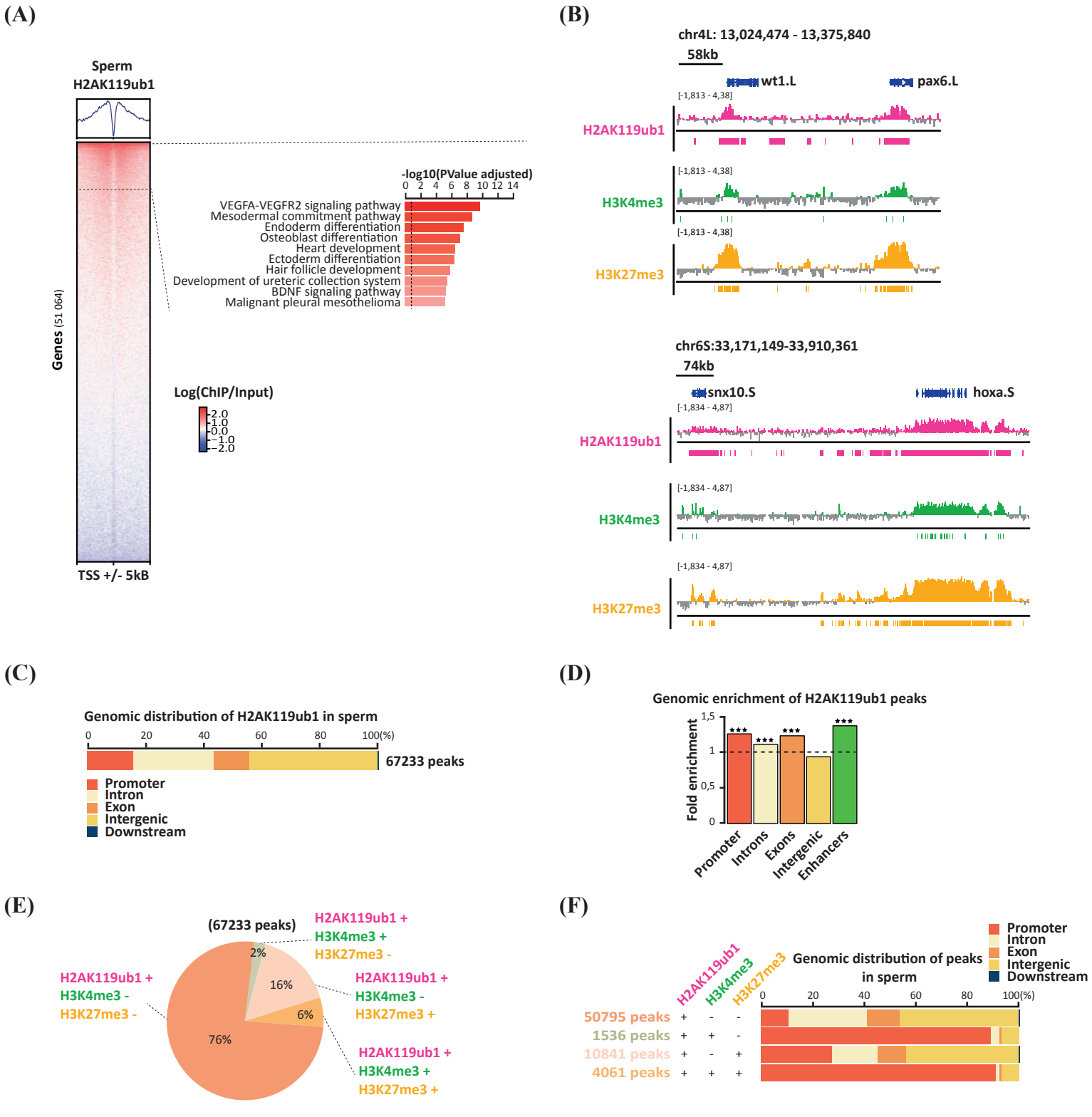
(A)
Sperm
H2AK119ub1
Genes (51 064)
TSS +/- 5kB
-log10(PValue adjusted)
0 2 4 6 8 10 12 14
VEGFA-VEGFR2 signaling pathway
Mesodermal commitment pathway
Endoderm differentiation
Osteoblast differentiation
Heart development
Ectoderm differentiation
Hair follicle development
Development of ureteric collection system
BDNF signaling pathway
Malignant pleural mesothelioma
Log(ChIP/Input)
2.0
1.0
0.0
-1.0
-2.0
(B)
chr4L: 13,024,474 - 13,375,840
58kb
wt1.L
pax6.L
H2AK119ub1
H3K4me3
H3K27me3
[-1,813 - 4,38]
chr6S:33,171,149-33,910,361
74kb
snx10.S
hoxa.S
[-1,834 - 4,87]
(C)
Genomic distribution of H2AK119ub1 in sperm
0 20 40 60 80 100(%)
67233 peaks
Promoter
Intron
Exon
Intergenic
Downstream
(D)
Genomic enrichment of H2AK119ub1 peaks
Fold enrichment
1,5
1
0,5
0
Promoter
Introns
Exons
Intergenic
Enhancers
(E)
(67233 peaks)
H2AK119ub1 +
H3K4me3 +
H3K27me3 -
2%
16%
6%
76%
H2AK119ub1 +
H3K4me3 -
H3K27me3 -
H2AK119ub1 +
H3K4me3 -
H3K27me3 +
H2AK119ub1 +
H3K4me3 +
H3K27me3 +
(F)
H2AK119ub1
H3K4me3
H3K27me3
Genomic distribution of peaks in sperm
Promoter
Intron
Exon
Intergenic
Downstream
0 20 40 60 80 100(%)
50795 peaks + - -
1536 peaks + + -
10841 peaks + - +
4061 peaks + + +

FIGURE 2

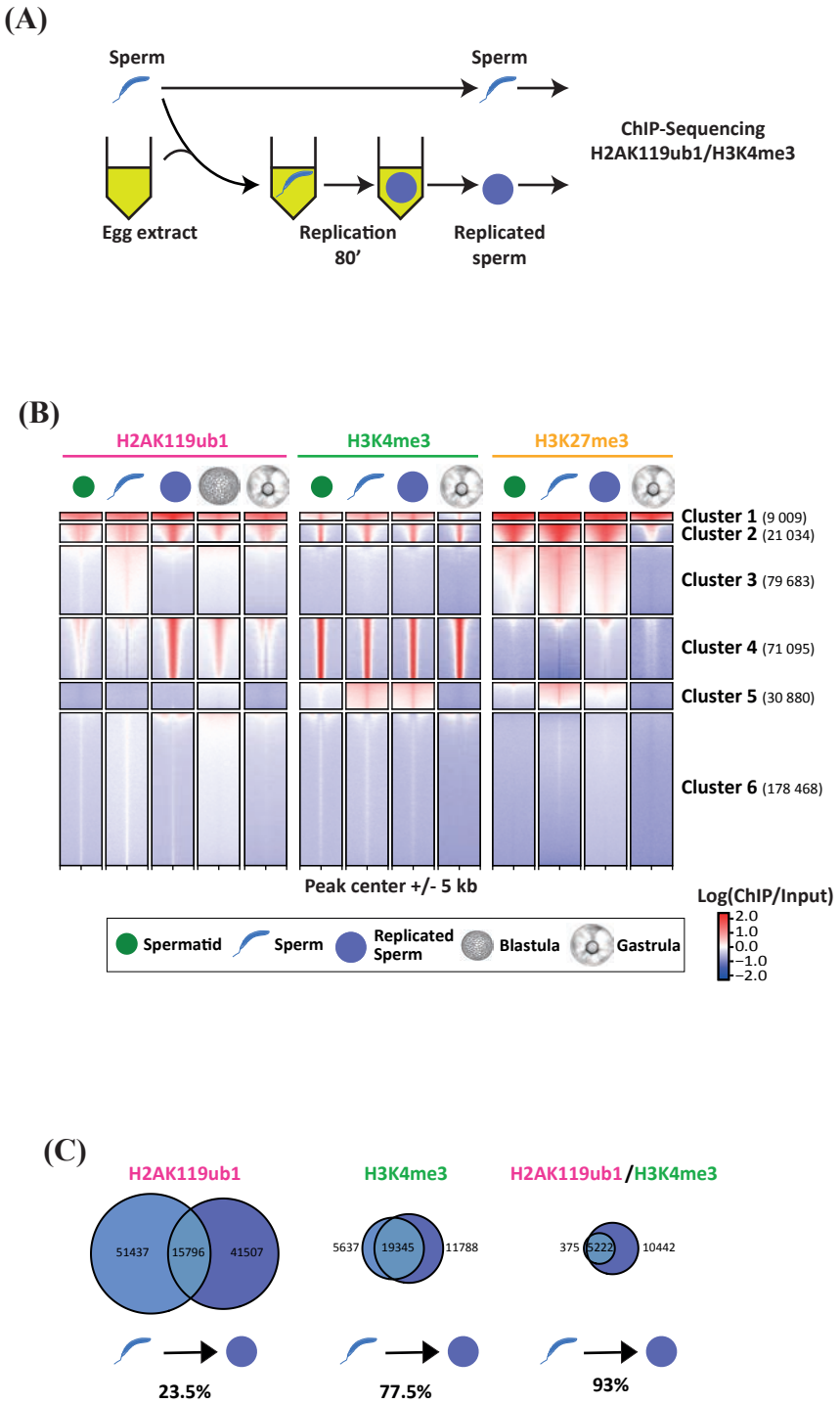
(A)
Sperm
Sperm
ChIP-Sequencing
H2AK119ub1/H3K4me3
Egg extract
Replication
80'
Replicated
sperm
(B)
H2AK119ub1
H3K4me3
H3K27me3
Cluster 1 (9 009)
Cluster 2 (21 034)
Cluster 3 (79 683)
Cluster 4 (71 095)
Cluster 5 (30 880)
Cluster 6 (178 468)
Peak center +/- 5 kb
Log(ChIP/Input)
2.0
1.0
0.0
−1.0
−2.0
Spermatid
Sperm
Replicated
Sperm
Blastula
Gastrula
(C)
H2AK119ub1
H3K4me3
H2AK119ub1/H3K4me3
51437
15796
41507
5637
19345
11788
375
5222
10442
23.5%
77.5%
93%

FIGURE 3

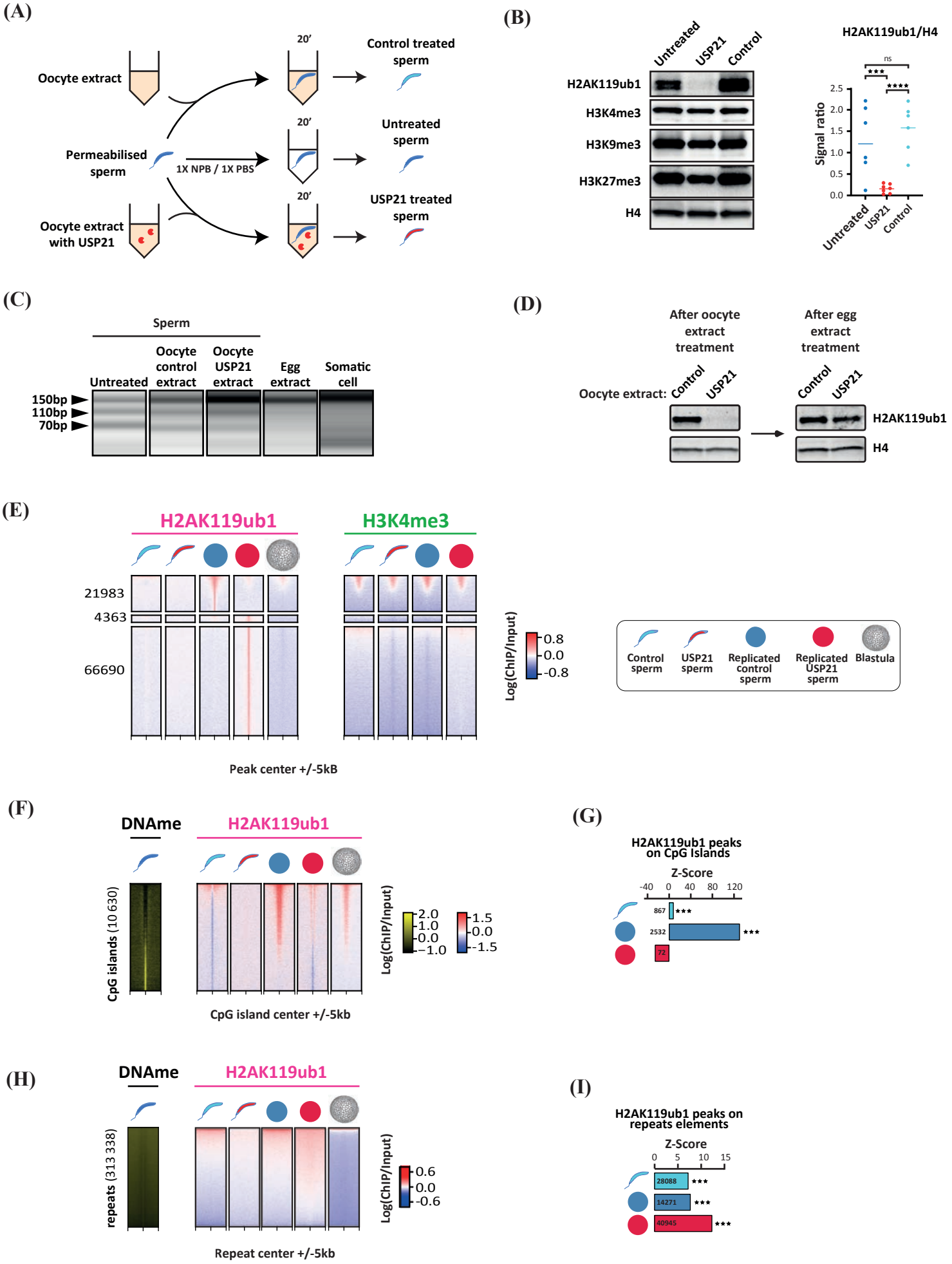
(A)
Oocyte extract
Permeabilised sperm
1X NPB / 1X PBS
Oocyte extract with USP21
20'
Control treated sperm
Untreated sperm
USP21 treated sperm
(B)
Untreated
USP21
Control
H2AK119ub1
H3K4me3
H3K9me3
H3K27me3
H4
H2AK119ub1/H4
Signal ratio
ns
***
****
(C)
Sperm
Untreated
Oocyte control extract
Oocyte USP21 extract
Egg extract
Somatic cell
150bp
110bp
70bp
(D)
After oocyte extract treatment
After egg extract treatment
Oocyte extract:
Control
USP21
H2AK119ub1
H4
(E)
H2AK119ub1
H3K4me3
21983
4363
66690
Log(ChIP/Input)
Peak center +/-5kB
Control sperm
USP21 sperm
Replicated control sperm
Replicated USP21 sperm
Blastula
(F)
DNAme
H2AK119ub1
CpG islands (10 630)
Log(ChIP/Input)
CpG island center +/-5kb
(G)
H2AK119ub1 peaks on CpG Islands
Z-Score
867
2532
72
(H)
DNAme
H2AK119ub1
repeats (313 338)
Log(ChIP/Input)
Repeat center +/-5kb
(I)
H2AK119ub1 peaks on repeats elements
Z-Score
28088
14271
40945

FIGURE 4

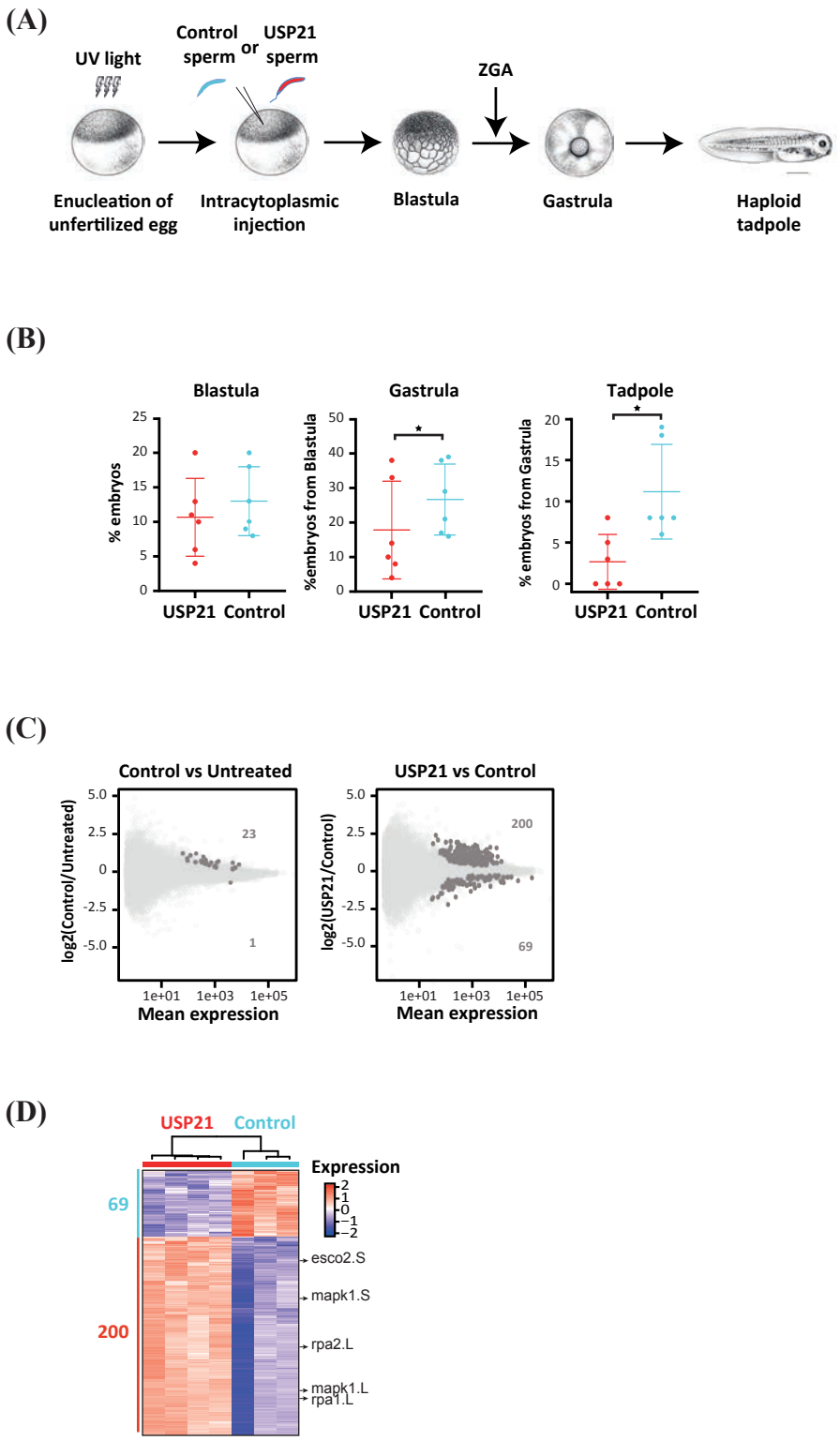
(A)
UV light
Control sperm
or
USP21 sperm
ZGA
Enucleation of unfertilized egg
Intracytoplasmic injection
Blastula
Gastrula
Haploid tadpole
(B)
Blastula
Gastrula
Tadpole
% embryos
%embryos from Blastula
% embryos from Gastrula
USP21
Control
(C)
Control vs Untreated
USP21 vs Control
log2(Control/Untreated)
log2(USP21/Control)
23
1
200
69
Mean expression
(D)
USP21
Control
Expression
69
200
esco2.S
mapk1.S
rpa2.L
mapk1.L
rpa1.L

FIGURE 5

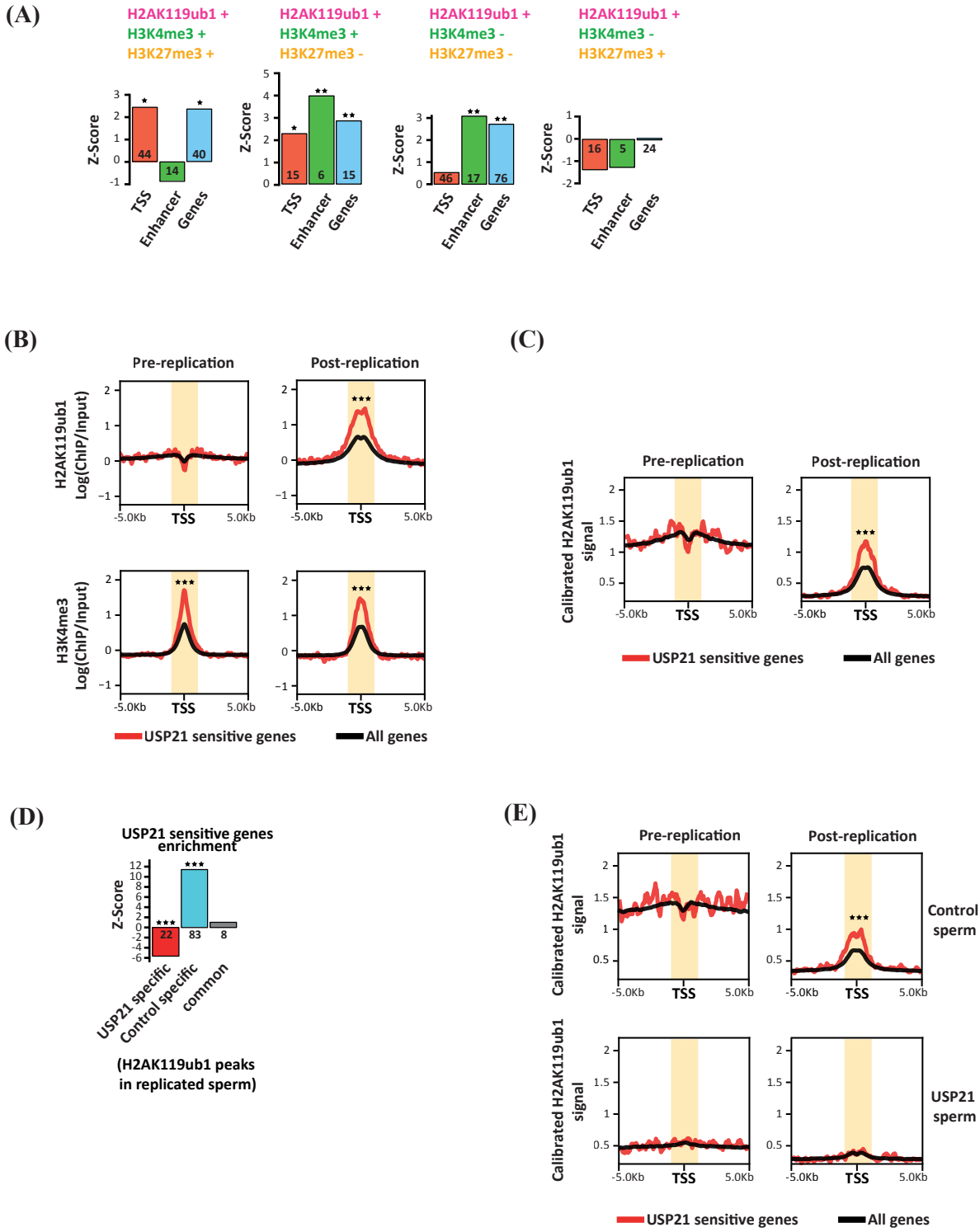
(A)
H2AK119ub1 +
H3K4me3 +
H3K27me3 +
H2AK119ub1 +
H3K4me3 +
H3K27me3 -
H2AK119ub1 +
H3K4me3 -
H3K27me3 -
H2AK119ub1 +
H3K4me3 -
H3K27me3 +
Z-Score
TSS
Enhancer
Genes
(B)
Pre-replication
Post-replication
H2AK119ub1 Log(ChIP/Input)
H3K4me3 Log(ChIP/Input)
-5.0Kb
5.0Kb
USP21 sensitive genes
All genes
(C)
Calibrated H2AK119ub1 signal
(D)
USP21 sensitive genes enrichment
USP21 specific
Control specific
common
(H2AK119ub1 peaks in replicated sperm)
(E)
Control sperm
USP21 sperm

FIGURE 6

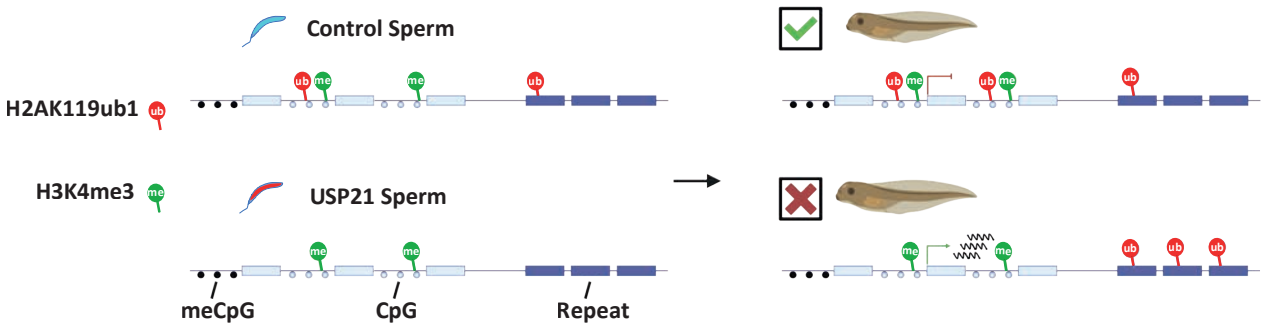
Control Sperm
H2AK119ub1
H3K4me3
USP21 Sperm
meCpG
CpG
Repeat

FIGURE 7